Hindawi
Computational and Mathematical Methods
Volume 2022, Article ID 2836545, 24 pages
https://doi.org/10.1155/2022/2836545

Research Article

Harmonic Mixture Weibull-G Family of Distributions: Properties, Regression and Applications to Medical Data

Ernest Zamanah,[1,2] **Suleman Nasiru**,[1] **and Albert Luguterah**[2]

[1]*Department of Statistics, School of Mathematical Sciences, C. K. Tedam University of Technology and Applied Sciences, Ghana*
[2]*Department of Biometry, School of Mathematical Sciences, C. K. Tedam University of Technology and Applied Sciences, Ghana*

Correspondence should be addressed to Ernest Zamanah; ezamanah@yahoo.com

Received 13 October 2022; Revised 9 November 2022; Accepted 16 November 2022; Published 28 November 2022

Academic Editor: Christophe Chesneau

In recent years, the developments of new families of probability distributions have received greater attention as a result of desirable properties they exhibit in the modelling of data sets. The Harmonic Mixture Weibull-G family of distributions was developed in this study. The statistical properties were comprehensively presented and five special distributions developed from the family. The hazard functions of the special distributions were shown to exhibit various forms of monotone and nonmonotone shapes. The applications of the developed family to real data sets in medical studies revealed that the special distribution (Harmonic mixture Weibul Weibull distribution) provided a better fit to the data sets than other competitive models. A location-scale regression model was developed from the family and its application demonstrated using survival time data of hypertensive patients.

1. Introduction

Advances in the field of medicine are critical to the well-being of humankind. To this end, the need for the use of appropriate and very efficient probability distributions in the modelling of medical data is fundamentally important. The efficient modelling of medical data is useful in providing good understanding of the distribution of disease incidence and prevalence in medical studies.

In medical and biological studies, several phenotypic traits including chronic conditions such as cancer, diabetes, hypertension, and cardiovascular diseases among others are usually encountered. Appropriate knowledge about the distribution of disease incidence and prevalence in a population enhances the development of appropriate hypotheses about underlying mechanisms of health and disease [1]. This is profoundly important in advancing the course of medicine.

In medical and biological studies, the Weibull distribution among numerous classical distributions is a widely applied model for analyzing data with monotone hazard rate shapes. For complex biological phenotypic traits with nonmonotone hazard rate shapes, the Weibull distribution does not have the flexibility to model such data. Consequently, new families of distributions in the form of extended or modified versions of the Weibull distribution have been introduced in literature with the attempt of increasing its flexibility. Some examples include the following: Marshall-Olkin Weibull generated family [2], exponentiated power generalized Weibull power series family of distributions [3], complementary generalized power Weibull power series family of distributions [4], the Burr-Weibull power series family [5], extended Weibull-G family [6], Weibull Burr X–G family of distributions [7], the Weibull Marshall–Olkin family [8], the gamma-Weibull-G family [9], generalized odd Weibull generated family [10], the beta Weibull-G family [11], Kumaraswamy Weibull-generated family [12], generalized extended Weibull power series family of distributions [13], the inverse Weibull power series family [14], the Marshall-Olkin extended Weibull

family of distributions, [15] and the extended Weibull power series family [16].

In this study, we proposed a novel generalization for the Weibull-G family, called the Harmonic mixture Weibull-G family by combining the Harmonic mixture-G [17] and the Weibull-G [18] families. The major motivations behind generating this family include the following: to develop special distributions capable of modelling medical data that are characterized with bimodality; to generate distributions with the capability of modelling medical data that are characterized with both monotone and nonmonotone hazard rate shapes; to produce special distributions that can generalize some well-known models in the literature; to generate more flexible distributions that take into consideration skewness, kurtosis, and tail variations in the modelling of medical data; to develop alternative distributions with superior parametric fits to data in medical studies than existing classical distributions; and to develop a location-scale regression model for studying the relationship between a response variable and a set of covariates.

The remainder of the article is structured as follows: Section 2 presents the development of the new family. Section 3 presents some statistical properties of the family. Section 4 presents the maximum likelihood estimation of the parameters. Section 5 presents some special distributions. Section 6 presents the location-scale regression model. Section 7 presents simulation results. Section 8 presents the applications of the developed family. Section 9 finally presents the conclusions of the study.

2. Development of the Harmonic Mixture Weibull-G Family

Suppose that the continuous random variable X follows the Weibull-G family of distributions. Then, according to Bourguignon et al. [18], the cumulative distribution function (CDF) and probability density function (PDF) are, respectively, given by

$$F(x) = 1 - \exp\left[-\alpha\left(\frac{G(x;\xi)}{\bar{G}(x;\xi)}\right)^{\beta}\right], x \in D \subseteq \mathbb{R}; \alpha, \beta > 0, \quad (1)$$

and

$$f(x;\alpha,\beta,\xi) = \alpha\beta g(x;\xi)\frac{G(x;\xi)^{\beta-1}}{\bar{G}(x;\xi)^{\beta+1}}\exp\left[-\alpha\left(\frac{G(x;\xi)}{\bar{G}(x;\xi)}\right)^{\beta}\right]. \quad (2)$$

If the random variable X follows the Harmonic mixture-G (HM-G) family, then according to Kharazmi et al. [17], the CDF and PDF are, respectively, given by

$$H(x) = 1 - \frac{\bar{G}^{\alpha}(x)}{1-\theta\left(1-\bar{G}^{\alpha-1}(x)\right)}, x \in \mathbb{R}, \alpha \geq 0, 0 < \theta < 1, \quad (3)$$

and

$$h(x) = g(x)\bar{G}^{\alpha-1}(x)\frac{\alpha(1-\theta)+\theta\bar{G}^{\alpha-1}(x)}{\left[1-\theta\left(1-\bar{G}^{\alpha-1}(x)\right)\right]^2}, x \in \mathbb{R}. \quad (4)$$

The Harmonic mixture Weibull generated (HMW-G) family of distributions is developed in this section by combining the CDFs of the HM-G and Weibull-G families. Suppose that the random variable X follows the HMW-G family of distributions, the CDF of the HMW-G family is given by

$$F_X(x) = 1 - \frac{\exp\left[-\alpha\left(G(x;\boldsymbol{\varphi})/\bar{G}(x;\boldsymbol{\varphi})\right)^{\beta}\right]}{1-\theta\left\{1-\left[\exp\left(-(\alpha-1)\left(G(x;\boldsymbol{\varphi})/\bar{G}(x;\boldsymbol{\varphi})\right)^{\beta}\right)\right]\right\}}, x \in \mathbb{R}, \quad (5)$$

where $\alpha > 0$ and $0 < \theta < 1$ are scale parameters, $\beta > 0$ is a shape parameter, and $\boldsymbol{\varphi}$ is a $p \times 1$ vector of parameters. When $\alpha = 0$, the HMW-G family reduces to the Marshall-Olkin Weibull-G family of distributions. The corresponding PDF of the HMW-G family is the first derivative of its CDF. Thus, the PDF is given by

$$f_X(x) = \beta g(x;\boldsymbol{\varphi})\frac{G(x;\boldsymbol{\varphi})^{\beta-1}}{\bar{G}(x;\boldsymbol{\varphi})^{\beta+1}}\exp\left[-\alpha\left(\frac{G(x;\boldsymbol{\varphi})}{\bar{G}(x;\boldsymbol{\varphi})}\right)^{\beta}\right]\frac{\alpha(1-\theta)+\theta\exp\left[-(\alpha-1)\left(G(x;\boldsymbol{\varphi})/\bar{G}(x;\boldsymbol{\varphi})\right)^{\beta}\right]}{\left\{1-\theta\left[1-\exp\left(-(\alpha-1)\left(G(x;\boldsymbol{\varphi})/\bar{G}(x;\boldsymbol{\varphi})\right)^{\beta}\right)\right]\right\}^2}, x \in \mathbb{R}. \quad (6)$$

The hazard rate function of the family is given by

$$r_X(x) = \beta g(x;\varphi)\frac{G(x;\varphi)^{\beta-1}}{\bar{G}(x;\varphi)^{\beta+1}}\frac{\alpha(1-\theta)+\theta\exp\left[-(\alpha-1)\left(G(x;\boldsymbol{\varphi})/\bar{G}(x;\boldsymbol{\varphi})\right)^{\beta}\right]}{1-\theta\left[1-\exp\left(-(\alpha-1)\left(G(x;\boldsymbol{\varphi})/\bar{G}(x;\boldsymbol{\varphi})\right)^{\beta}\right)\right]}, x \in \mathbb{R}. \quad (7)$$

Lemma 1. *The mixture representation of the density function of the HMW-G family is*

$$f_X(x) = \beta\sum_{i=0}^{\infty}\sum_{j=0}^{i}\sum_{k=0}^{\infty}\sum_{m=0}^{\infty}\left(\bar{\omega}_{ijkm}+\omega_{ijkm}\right)g(x;\varphi)G(x;\varphi)^{\beta(k+1)+m-1}, \quad (8)$$

where

$$\bar{\omega}_{ijkm} = \frac{(-1)^{j+k}(i+1)[\alpha + j(\alpha-1)]^k \theta^i \alpha(1-\theta)}{k!} \binom{\beta(k+1)+m}{m},$$
$$\omega_{ijkm} = \frac{(-1)^{j+k}(i+1)\theta^{i+1}[2\alpha + j(\alpha-1)-1]^k}{k!} \binom{\beta(k+1)+m}{m}. \tag{9}$$

Proof. Using the binomial series expansion $(1-z)^{-n} = \sum_{i=0}^{\infty} \binom{n+i-1}{i} z^i, |z| < 1$,

$$\left\{1 - \theta\left[1 - e^{-(\alpha-1)\left(\frac{G(x;\boldsymbol{\varphi})}{\bar{G}(x;\boldsymbol{\varphi})}\right)^{\beta}}\right]\right\}^{-2} = \sum_{i=0}^{\infty}\sum_{j=0}^{i}(-1)^i(i+1)\theta^i e^{-j(\alpha-1)\left(\frac{G(x;\boldsymbol{\varphi})}{\bar{G}(x;\boldsymbol{\varphi})}\right)^{\beta}}. \tag{10}$$

Thus, the PDF of the HMW-G family can be written as

$$f_X(x) = \beta g(x;\boldsymbol{\varphi})\frac{G(x;\boldsymbol{\varphi})^{\beta-1}}{\bar{G}(x;\boldsymbol{\varphi})^{\beta+1}}\sum_{i=0}^{\infty}\sum_{j=0}^{i}(-1)^j(i+1)\,\theta^i\alpha(1-\theta)e^{-[\alpha+j(\alpha-1)]\left(\frac{G(x;\boldsymbol{\varphi})}{\bar{G}(x;\boldsymbol{\varphi})}\right)^{\beta}} + \beta g(x;\boldsymbol{\varphi})\frac{G(x;\boldsymbol{\varphi})^{\beta-1}}{\bar{G}(x;\boldsymbol{\varphi})^{\beta+1}}\sum_{i=0}^{\infty}\sum_{j=0}^{i}(-1)^j(i+1)\theta^{i+1}e^{-[2\alpha+j(\alpha-1)-1]\left(\frac{G(x;\boldsymbol{\varphi})}{\bar{G}(x;\boldsymbol{\varphi})}\right)^{\beta}}. \tag{11}$$

Using the Taylor series, we have

$$f_X(x) = \beta g(x;\boldsymbol{\varphi})\sum_{i=0}^{\infty}\sum_{j=0}^{i}\sum_{k=0}^{\infty}\frac{(-1)^{j+k}(i+1)[\alpha+j(\alpha-1)]^k\theta^i\alpha(1-\theta)}{k!}\frac{G(x;\boldsymbol{\varphi})^{\beta(k+1)-1}}{\bar{G}(x;\boldsymbol{\varphi})^{\beta(k+1)+1}} + \beta g(x;\boldsymbol{\varphi})\sum_{i=0}^{\infty}\sum_{j=0}^{i}\sum_{k=0}^{\infty}\frac{(-1)^{j+k}(i+1)[2\alpha+j(\alpha-1)-1]^k\theta^{i+1}}{k!}\frac{G(x;\boldsymbol{\varphi})^{\beta(k+1)-1}}{\bar{G}(x;\boldsymbol{\varphi})^{\beta(k+1)+1}}. \tag{12}$$

Applying the binomial series expansion,

$$f_X(x) = \beta g(x;\boldsymbol{\varphi})\sum_{i=0}^{\infty}\sum_{j=0}^{i}\sum_{k=0}^{\infty}\sum_{m=0}^{\infty}\frac{(-1)^{j+k}(i+1)[\alpha+j(\alpha-1)]^k\theta^i\alpha(1-\theta)}{k!} \cdot \binom{\beta(k+1)+m}{m}G(x;\boldsymbol{\varphi})^{\beta(k+1)+m-1} + \beta g(x;\boldsymbol{\varphi})\sum_{i=0}^{\infty}\sum_{j=0}^{i}\sum_{k=0}^{\infty}\sum_{m=0}^{\infty}\frac{(-1)^{j+k}(i+1)[2\alpha+j(\alpha-1)-1]^k\theta^{i+1}}{k!} \cdot \binom{\beta(k+1)+m}{m}G(x;\boldsymbol{\varphi})^{\beta(k+1)+m-1}. \tag{13}$$

Thus,

$$f_X(x) = \beta\sum_{i=0}^{\infty}\sum_{j=0}^{i}\sum_{k=0}^{\infty}\sum_{m=0}^{\infty}(\bar{\omega}_{ijkm} + \omega_{ijkm})g(x;\boldsymbol{\varphi})G(x;\boldsymbol{\varphi})^{\beta(k+1)+m-1}. \tag{14}$$

This completes the proof. □

3. Statistical Properties

In this section, statistical properties of the HMW-G family of distributions are presented.

3.1. Quantile Function. The quantile function plays an important role in simulating random samples from a given distribution. For a given distribution, the characteristics such as median, kurtosis, and skewness can also be described using the quantile function.

Proposition 2. *The quantile function of the HMW-G family for $u \in [0, 1]$ is given by*

$$(1-u)\left\{1 - \theta\left[\exp\left(-(\alpha-1)\left(\frac{G(x;\varphi)}{\bar{G}(x;\varphi)}\right)^{\beta}\right)\right]\right\} - \exp\left[-\alpha\left(\frac{G(x;\varphi)}{\bar{G}(x;\varphi)}\right)^{\beta}\right] = 0. \tag{15}$$

Proof. Using the CDF of the HMW-G family defined in equation (5), let U be a random variable having the uniform distribution on the interval [0, 1]. Then, the u^{th} quantile, denoted by x_u is obtained such that,

$$1 - \frac{\exp\left[-\alpha\left(G(x;\varphi)/\bar{G}(x;\varphi)\right)^{\beta}\right]}{1-\theta\left\{1 - \left[\exp\left(-(\alpha-1)\left(G(x;\varphi)/\bar{G}(x;\varphi)\right)^{\beta}\right)\right]\right\}} = u. \tag{16}$$

This implies that

$$1 - \theta\left\{1 - \left[\exp\left(-(\alpha-1)\left(\frac{G(x;\varphi)}{\bar{G}(x;\varphi)}\right)^{\beta}\right)\right]\right\} - \exp\left\{-\alpha\left[\frac{G(x;\boldsymbol{\varphi})}{\bar{G}(x;\boldsymbol{\varphi})}\right]^{\beta}\right\} = u \left\{1 - \theta\left[1 - \left(\exp\left(-(\alpha-1)\left(\frac{G(x;\varphi)}{\bar{G}(x;\varphi)}\right)^{\beta}\right)\right)\right]\right\}. \tag{17}$$

Hence, the quantile is obtained as the solution of

$$(1-u)\left\{1-\theta\left[1-\left(\exp\left(-(\alpha-1)\left(\frac{G(x;\varphi)}{\bar{G}(x;\varphi)}\right)^{\beta}\right)\right)\right]\right\} - \exp\left[-\alpha\left(\frac{G(x;\varphi)}{\bar{G}(x;\varphi)}\right)^{\beta}\right]=0. \tag{18}$$

This completes the proof. □

3.2. Moments. In this section, the expression for the r^{th} order moment of the HMW-G family of distributions is derived. It can be used to compute measures of dispersion, kurtosis, and skewness of data sets in medical studies.

Proposition 3. *The r^{th} noncentral moment of the HMW-G family of distributions is*

$$\mu_r' = \beta\sum_{i=0}^{\infty}\sum_{j=0}^{i}\sum_{k=0}^{\infty}\sum_{m=0}^{\infty}\left(\bar{\omega}_{ijkm}+\omega_{ijkm}\right)\int_{-\infty}^{\infty}x^r g(x;\boldsymbol{\varphi})G(x;\boldsymbol{\varphi})^{\beta(k+1)+m-1}dx,\ r=1,2,.\cdots \tag{19}$$

Proof. The r^{th} noncentral moment is defined as

$$\mu_r' = \int_{-\infty}^{\infty}x^r f_X(x)dx. \tag{20}$$

Substituting the mixture representation of the density function into the definition, we have

$$\mu_r' = \int_{-\infty}^{\infty}x^r\beta\sum_{i=0}^{\infty}\sum_{j=0}^{i}\sum_{k=0}^{\infty}\sum_{m=0}^{\infty}\left(\bar{\omega}_{ijkm}+\omega_{ijkm}\right)g(x;\boldsymbol{\varphi})G(x;\boldsymbol{\varphi})^{\beta(k+1)+m-1}dx. \tag{21}$$

This implies that

$$\mu_r' = \beta\sum_{i=0}^{\infty}\sum_{j=0}^{i}\sum_{k=0}^{\infty}\sum_{m=0}^{\infty}\left(\bar{\omega}_{\mathrm{ijkm}}+\omega_{\mathrm{ijkm}}\right)\int_{-\infty}^{\infty}x^r g(x;\boldsymbol{\varphi})G(x;\boldsymbol{\varphi})^{\beta(k+1)+m-1}\mathrm{dx},\ r=1,2,.\cdots \tag{22}$$

This completes the proof. □

3.3. Incomplete Moment. In this section, the expression for the r^{th} incomplete moment of the HMW-G family of distributions is derived. It can be used to determine the mean deviation or median deviation of data sets in medical studies.

Proposition 4. *The r^{th} incomplete moment of the HMW-G family of distributions is*

$$\psi_r(y) = \beta\sum_{i=0}^{\infty}\sum_{j=0}^{i}\sum_{k=0}^{\infty}\sum_{m=0}^{\infty}\left(\bar{\omega}_{ijkm}+\omega_{ijkm}\right)\int_{-\infty}^{y}x^r g(x;\boldsymbol{\varphi})G(x;\boldsymbol{\varphi})^{\beta(k+1)+m-1}dx,\ r=1,2,.\cdots \tag{23}$$

Proof. By definition, the r^{th} incomplete moment is given by

$$\psi_r(y) = E(X|X<Y) = \int_{-\infty}^{y}x^r f_X(x)dx. \tag{24}$$

Substituting the mixture representation of the density function into the definition, we have

$$\psi_r(y) = \int_{-\infty}^{y}x^r\beta\sum_{i=0}^{\infty}\sum_{j=0}^{i}\sum_{k=0}^{\infty}\sum_{m=0}^{\infty}\left(\bar{\omega}_{ijkm}+\omega_{ijkm}\right)g(x;\boldsymbol{\varphi})G(x;\boldsymbol{\varphi})^{\beta(k+1)+m-1}dx. \tag{25}$$

This implies that

$$\psi_r(y) = \beta\sum_{i=0}^{\infty}\sum_{j=0}^{i}\sum_{k=0}^{\infty}\sum_{m=0}^{\infty}\left(\bar{\omega}_{ijkm}+\omega_{ijkm}\right)\int_{-\infty}^{y}x^r g(x;\boldsymbol{\varphi})G(x;\boldsymbol{\varphi})^{\beta(k+1)+m-1}dx,\ r=1,2,.\cdots \tag{26}$$

□

3.4. Moment Generating Function. In this section, the expression for the moment generating function (MGF) of the HMW-G family of distributions is presented. The MGF is useful in finding the moments of a random variable. The MGF of a random variable X having the HMW-G distribution if it exists is given by the following proposition.

Proposition 5. *The MGF of the HMW-G family of distribution is given by*

$$M_X(t) = \beta\sum_{r=0}^{\infty}\sum_{i=0}^{\infty}\sum_{j=0}^{i}\sum_{k=0}^{\infty}\sum_{m=0}^{\infty}\left(\bar{\omega}_{ijkm}+\omega_{ijkm}\right)\frac{t^r}{r!}\int_{-\infty}^{\infty}g(x;\boldsymbol{\varphi})G(x;\boldsymbol{\varphi})^{\beta(k+1)+m-1}dx,\ r=1,2,.\cdots \tag{27}$$

Proof. By definition, the MGF is given by

$$M_X(t) = E\left(e^{tX}\right) = \int_{-\infty}^{\infty}e^{tx}f_X(x)dx. \tag{28}$$

Using the Taylor series expansion,

$$e^{tX} = \sum_{r=0}^{\infty}\frac{t^r X^r}{r!}. \tag{29}$$

This implies that

$$M_X(t) = E\left(\sum_{r=0}^{\infty}\frac{t^r X^r}{r!}\right) = \sum_{r=0}^{\infty}\frac{t^r}{r!}E(X^r) = \sum_{r=0}^{\infty}\frac{t^r}{r!}\mu_r'. \tag{30}$$

Substituting μ_r' into equation (30) gives

$$M_X(t) = \beta \sum_{r=0}^{\infty}\sum_{i=0}^{\infty}\sum_{j=0}^{i}\sum_{k=0}^{\infty}\sum_{m=0}^{\infty}(\bar{\omega}_{ijkm}+\omega_{ijkm})\frac{t^r}{r!}\int_{-\infty}^{\infty} g(x;\boldsymbol{\varphi})G(x;\boldsymbol{\varphi})^{\beta(k+1)+m-1}dx,\ r=1,2,.\cdots \tag{31}$$

This completes the proof. □

3.5. Mean Residual Life. The Mean Residual Life (MRL) function $m(y)$, is a function that characterizes the distribution function $F(y)$, uniquely [19]. It describes the average survival time of a component after it exceeds a specific time$y$. The MRL function plays a key role in survival analysis when analyzing the event time of a given phenotypic trait in medical studies.

Proposition 6. *If Y is a random variable representing the life time of a component with distribution function $F(y)$, then the MRL of the HMW-G family of distributions is*

$$m(y) = \frac{\mu - \beta\sum_{i=0}^{\infty}\sum_{j=0}^{i}\sum_{k=0}^{\infty}\sum_{m=0}^{\infty}(\bar{\omega}_{ijkm}+\omega_{ijkm})\int_{-\infty}^{y} xg(x;\boldsymbol{\varphi})G(x;\boldsymbol{\varphi})^{\beta(k+1)+m-1}dx}{1-F_X(y)} - y, \tag{32}$$

where $\mu = \mu_1'$..

Proof. By definition, the MRL is given by

$$\begin{aligned} m(y) &= E(X-y|X>y) = \frac{1}{1-F_X(y)}\int_y^{\infty}(x-y)f(x)dx \\ &= \frac{\mu_1' - \int_{-\infty}^{y} xf_X(x)dx}{1-F_X(y)} - y. \end{aligned} \tag{33}$$

Hence, substituting the first incomplete moment $\int_{-\infty}^{y} xf_X(x)dx$, into equation (33) gives

$$m(y) = \frac{\mu - \beta\sum_{i=0}^{\infty}\sum_{i=0}^{i}\sum_{k=0}^{\infty}\sum_{m=0}^{\infty}(\bar{\omega}_{ijkm}+\omega_{ijkm})\int_{-\infty}^{y}\int_{-\infty}^{y} xg(x;\boldsymbol{\varphi})G(x;\boldsymbol{\varphi})^{\beta(k+1)+m-1}dx}{1-F_X(y)} - y. \tag{34}$$

This completes the proof. □

3.6. Identifiability. The identifiability property of the HMW-G family is studied in this section. The identifiability property of the model is essential to ensure that precise inferences are possible.

Proposition 7. *Let X_1 be HMW-G family random variable with CDF $F_X(x;\alpha_1,\beta_1,\theta_1,\boldsymbol{\varphi}_1)$ and X_2 be HMW-G family random variable with CDF $F_X(x;\alpha_2,\beta_2,\theta_2,\boldsymbol{\varphi}_2)$. Then, the HMW-G family is identifiable if $\alpha_1=\alpha_2, \beta_1=\beta_2, \theta_1=\theta_2$ and $\boldsymbol{\varphi}_1=\boldsymbol{\varphi}_2$.*

Proof. For the HMW-G family of distributions to be identifiable, $F_X(x;\alpha_1,\beta_1,\theta_1,\boldsymbol{\varphi}_1) = F_X(x;\alpha_2,\beta_2,\theta_2,\boldsymbol{\varphi}_2)$.

Hence,

$$\begin{aligned} 1 - \frac{\exp\left[-\alpha_1\left(G(x;\boldsymbol{\varphi}_1)/\bar{G}(x;\boldsymbol{\varphi}_1)\right)^{\beta_1}\right]}{1-\theta_1\left\{1-\left[\exp\left(-(\alpha_1-1)\left(G(x;\boldsymbol{\varphi}_1)/\bar{G}(x;\boldsymbol{\varphi}_1)\right)^{\beta_1}\right)\right]\right\}} \\ = 1 - \frac{\exp\left[-\alpha_2\left(G(x;\boldsymbol{\varphi}_2)/\bar{G}(x;\boldsymbol{\varphi}_2)\right)^{\beta_2}\right]}{1-\theta_2\left\{1-\left[\exp\left(-(\alpha_2-1)\left(G(x;\boldsymbol{\varphi}_2)/\bar{G}(x;\boldsymbol{\varphi}_2)\right)^{\beta_2}\right)\right]\right\}}. \end{aligned} \tag{35}$$

If $\alpha_1=\alpha_2, \beta_1=\beta_2, \theta_1=\theta_2$ and $\boldsymbol{\varphi}_1=\boldsymbol{\varphi}_2$,

$$\begin{aligned} &\frac{\exp\left[-\alpha_2\left(G(x;\boldsymbol{\varphi}_2)/\bar{G}(x;\boldsymbol{\varphi}_2)\right)^{\beta_2}\right]}{1-\theta_2\left\{1-\left[\exp\left(-(\alpha_2-1)\left(G(x;\boldsymbol{\varphi}_2)/\bar{G}(x;\boldsymbol{\varphi}_2)\right)^{\beta_2}\right)\right]\right\}} \\ &- \frac{\exp\left[-\alpha_1\left(G(x;\boldsymbol{\varphi}_1)/\bar{G}(x;\boldsymbol{\varphi}_1)\right)^{\beta_1}\right]}{1-\theta_1\left\{1-\left[\exp\left(-(\alpha_1-1)\left(G(x;\boldsymbol{\varphi}_1)/\bar{G}(x;\boldsymbol{\varphi}_1)\right)^{\beta_1}\right)\right]\right\}} = 0. \end{aligned} \tag{36}$$

Hence, the identifiability condition is satisfied. This completes the proof. □

4. Parameter Estimation

In this section, the maximum likelihood estimation (MLE) procedure is presented for the estimation of the unknown parameters of the HMW-G family. Let $x_1, x_2, \cdots, x_n$ be a random sample of size n from the HMW-G family of distributions with $\Psi = (\alpha, \beta, \phi, \boldsymbol{\varphi})'$ an unknown parameter vector where $\boldsymbol{\varphi}$ is a $p \times 1$ parameter vector for the baseline distribution. Under these settings, the total log-likelihood function is

$$\begin{aligned} \ell &= n\log(\beta) + \sum_{i=1}^{n}\log g(x_i;\boldsymbol{\varphi}) + (\beta-1)\sum_{i=1}^{n}\log G(x_i;\boldsymbol{\varphi}) \\ &- (\beta+1)\sum_{i=1}^{n}\log\bar{G}(x_i;\boldsymbol{\varphi}) - \alpha\sum_{i=1}^{n}\left(\frac{G(x;\boldsymbol{\varphi})}{\bar{G}(x;\boldsymbol{\varphi})}\right)^{\beta} \\ &+ \sum_{i=1}^{n}\log\left\{\alpha(1-\theta) + \theta\exp\left[-(\alpha-1)\left(\frac{G(x;\boldsymbol{\varphi})}{\bar{G}(x;\boldsymbol{\varphi})}\right)^{\beta}\right]\right\} \\ &- 2\sum_{i=1}^{n}\log\left\{1-\theta\left[1-\exp\left(-(\alpha-1)\left(\frac{G(x;\boldsymbol{\varphi})}{\bar{G}(x;\boldsymbol{\varphi})}\right)^{\beta}\right)\right]\right\}. \end{aligned} \tag{37}$$

The score vectors $U(\Psi)$ of the likelihood function are obtained by taking partial derivatives of (35) with respect to the parameters α, β, θ and $\boldsymbol{\varphi}$ as

$$U(\Psi) = \frac{\partial\ell}{\partial\Psi} = \left(\frac{\partial\ell}{\partial\alpha}, \frac{\partial\ell}{\partial\beta}, \frac{\partial\ell}{\partial\theta}, \frac{\partial\ell}{\partial\boldsymbol{\varphi}}\right)'. \tag{38}$$

By setting the score vectors to zero, the simultaneous solution of the system of nonlinear equations gives the maximum likelihood estimates of the parameters. However, this nonlinear system of equations does not have a closed form.

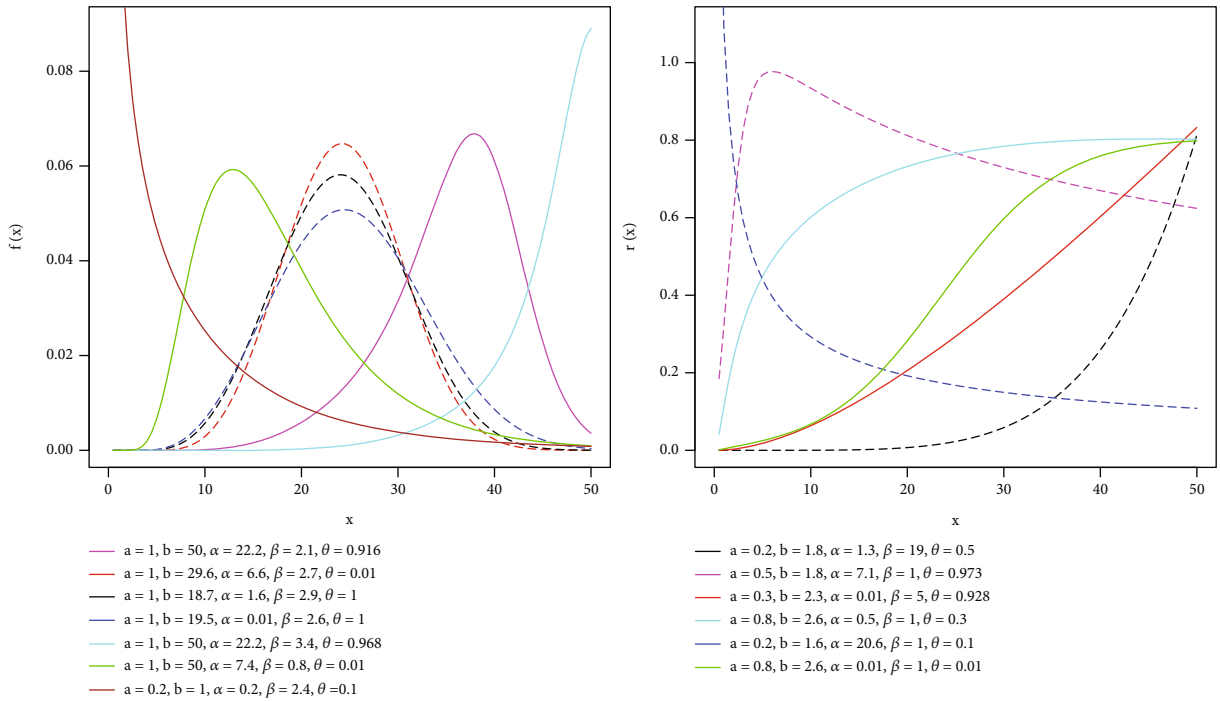

FIGURE 1: Plots of density and hazard rate functions of the HMWBIII distribution.

Thus, we apply numerical optimization to maximize the log-likelihood function directly using R software.

5. Special Distributions

In this section, some special cases of the HMW-G family of distributions are developed and studied.

5.1. Harmonic Mixture Weibull Burr III Distribution. Suppose that the baseline model of the HMW-G family is the Burr III distribution with CDF and PDF, respectively, defined by Burr [20] as $G(x) = (1 + x^{-a})^{-b}$ and $g(x) = abx^{-a-1}(1 + x^{-a})^{-b-1}, x > 0, a > 0, b > 0$. Then, the PDF and hazard function of the HMW-Burr III (HMWBIII) distribution are given, respectively, by

$$f_X(x) = \frac{\beta abx^{-a-1}(1+x^{-a})^{-(b\beta+1)} \exp\left\{-\alpha\left[(1+x^{-a})^{b}-1\right]^{-\beta}\right\}}{\left[1-(1+x^{-a})^{-b}\right]^{\beta+1}} \times \frac{\alpha(1-\theta)+\theta\exp\left\{-(\alpha-1)\left[(1+x^{-a})^{b}-1\right]^{-\beta}\right\}}{\left\{1-\theta\left[1-\exp\left(-(\alpha-1)\left((1+x^{-a})^{b}-1\right)^{-\beta}\right)\right]\right\}^{2}}, \tag{39}$$

where $x > 0, \alpha > 0, \beta > 0, 0 < \theta < 1, a > 0$ and $b > 0$, and

$$r(x) = \frac{\beta abx^{-a-1}(1+x^{-a})^{-(b\beta+1)}\left\{\alpha(1-\theta)+\theta\exp\left[-(\alpha-1)\left((1+x^{-a})^{b}-1\right)^{-\beta}\right]\right\}}{\left[1-(1+x^{-a})^{-b}\right]^{\beta+1}\left\{1-\theta\left[1-\exp\left(-(\alpha-1)\left((1+x^{-a})^{b}-1\right)^{-\beta}\right)\right]\right\}}, x > 0. \tag{40}$$

The density plot of the HMWBIII distribution exhibited a variety of shapes such as; reverse J-shape, J-shape, right skewed, various forms of symmetric, and left skewed shapes as shown in Figure 1. The hazard rate function also showed varied shapes such as; upside-down bathtub, monotone decreasing, and various forms of monotone increasing failure rates for some selected values.

The quantile function $Q_G(u)$ for the HMWBIII distribution is given by

$$(1-u)\left\{1-\theta\left[\exp\left(-(\alpha-1)\left((1+x^{-a})^{b}-1\right)^{-\beta}\right)\right]\right\} - \exp\left\{-\alpha\left[(1+x^{-a})^{b}-1\right]^{-\beta}\right\} = 0, u \in [0,1]. \tag{41}$$

5.2. Harmonic Mixture Weibull Lomax Distribution. Considering the Lomax distribution as the baseline model with CDF and PDF, respectively, defined by Lomax [21] as $G(x) = 1 - (1 + ax)^{-b}$ and $g(x) = ab(1 + ax)^{-(b+1)}, x > 0, a > 0, b > 0$, the PDF of the Harmonic mixture Weibull Lomax (HMWL) distribution is given by

$$f_X(x) = \beta ab(1+ax)^{b\beta-1}\left[1-(1+ax)^{-b}\right]^{\beta-1}\exp\left\{-\alpha\left[(1+ax)^{b}-1\right]^{\beta}\right\} \times \frac{\alpha(1-\theta)+\theta\exp\left\{-(\alpha-1)\left[(1+ax)^{b}-1\right]^{\beta}\right\}}{\left\{1-\theta\left[1-\exp\left(-(\alpha-1)\left((1+ax)^{b}-1\right)^{\beta}\right)\right]\right\}^{2}}, x > 0, \tag{42}$$

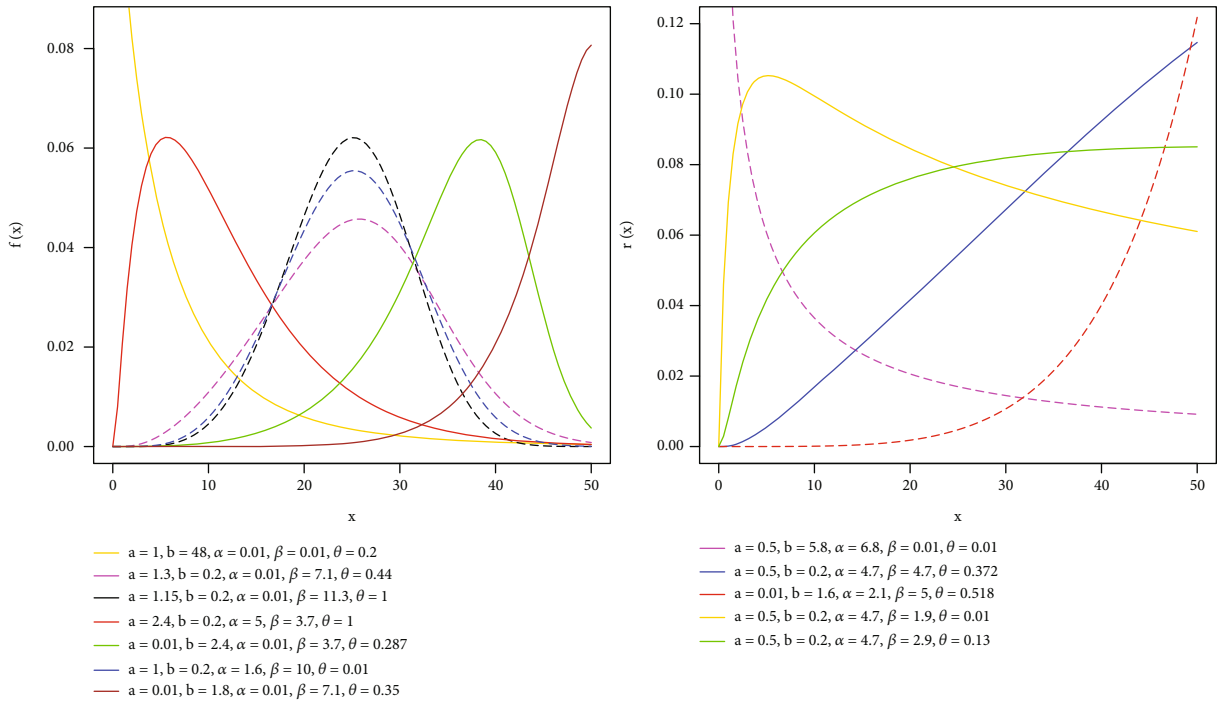

Figure 2: Plots of density and hazard rate functions of the HMWL distribution.

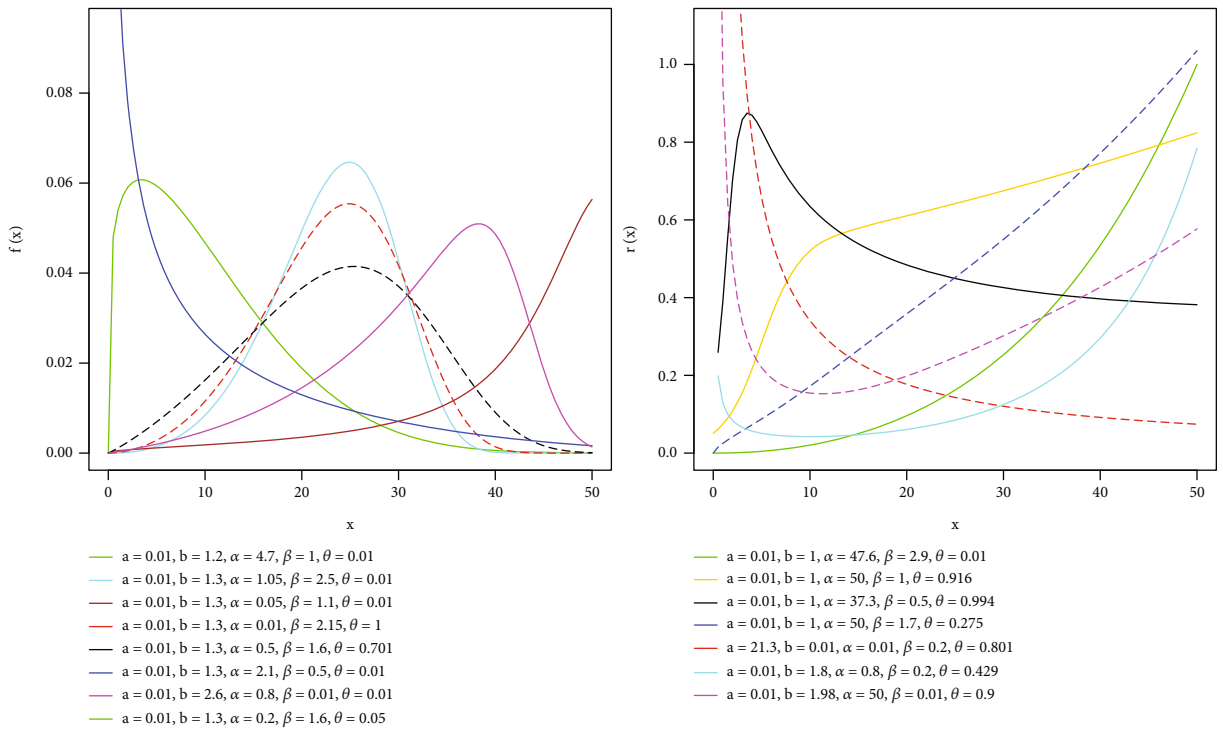

Figure 3: Plots of density and hazard rate functions of the HMWW distribution.

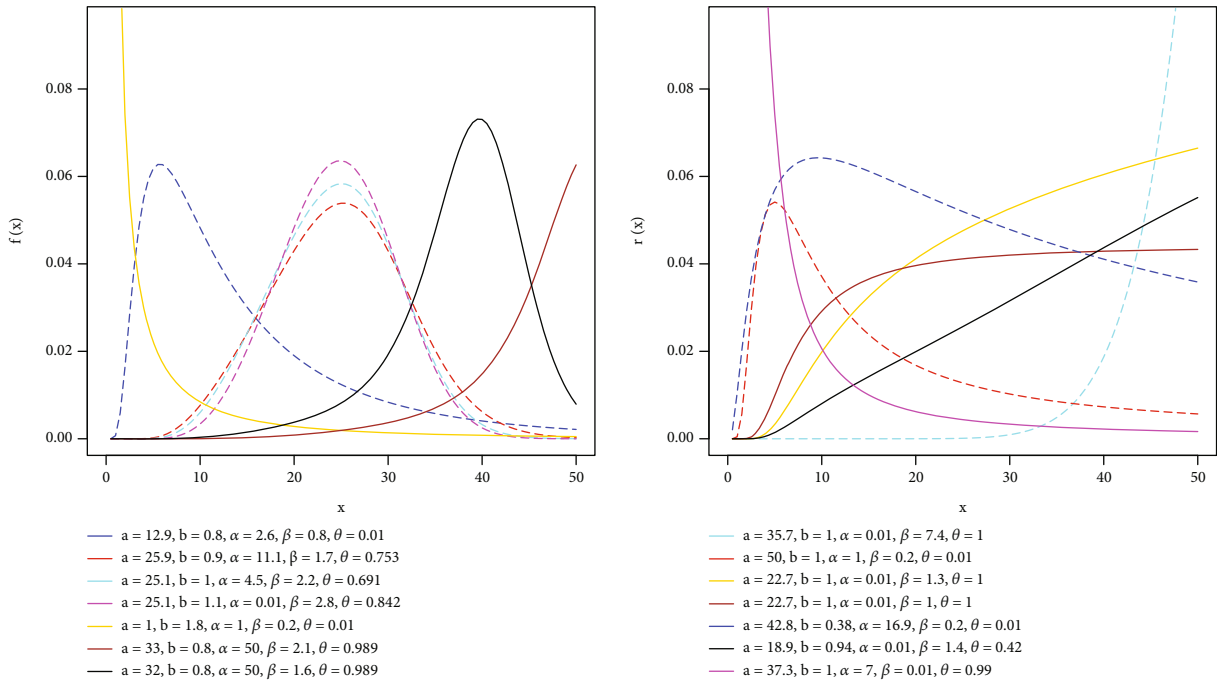

Figure 4: Plots of density and hazard rate functions of the HMWF distribution.

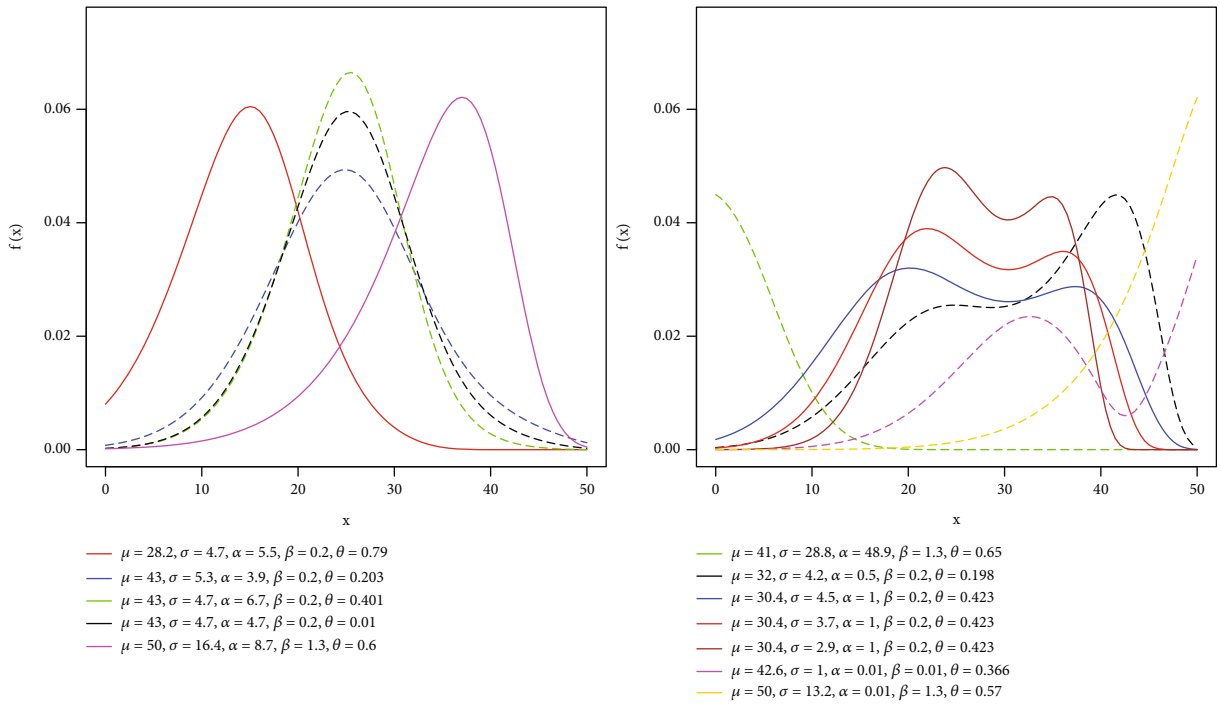

Figure 5: Plots of density function of the HMWN distribution.

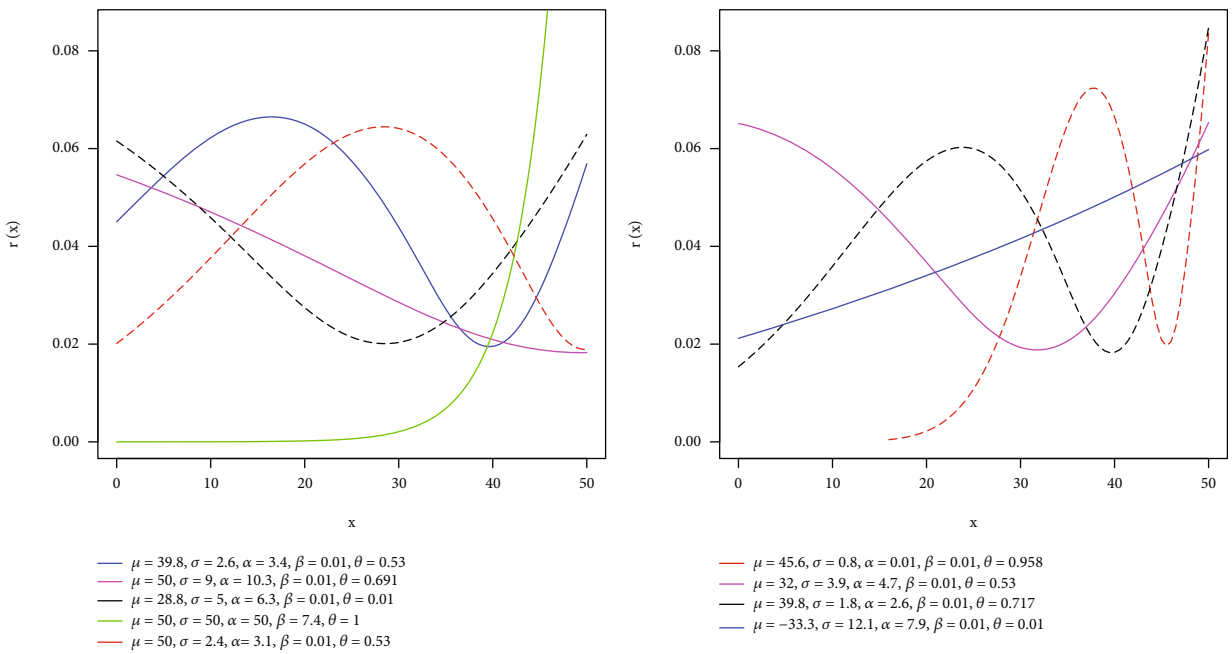

Figure 6: Plots of hazard rate function of the HMWN distribution.

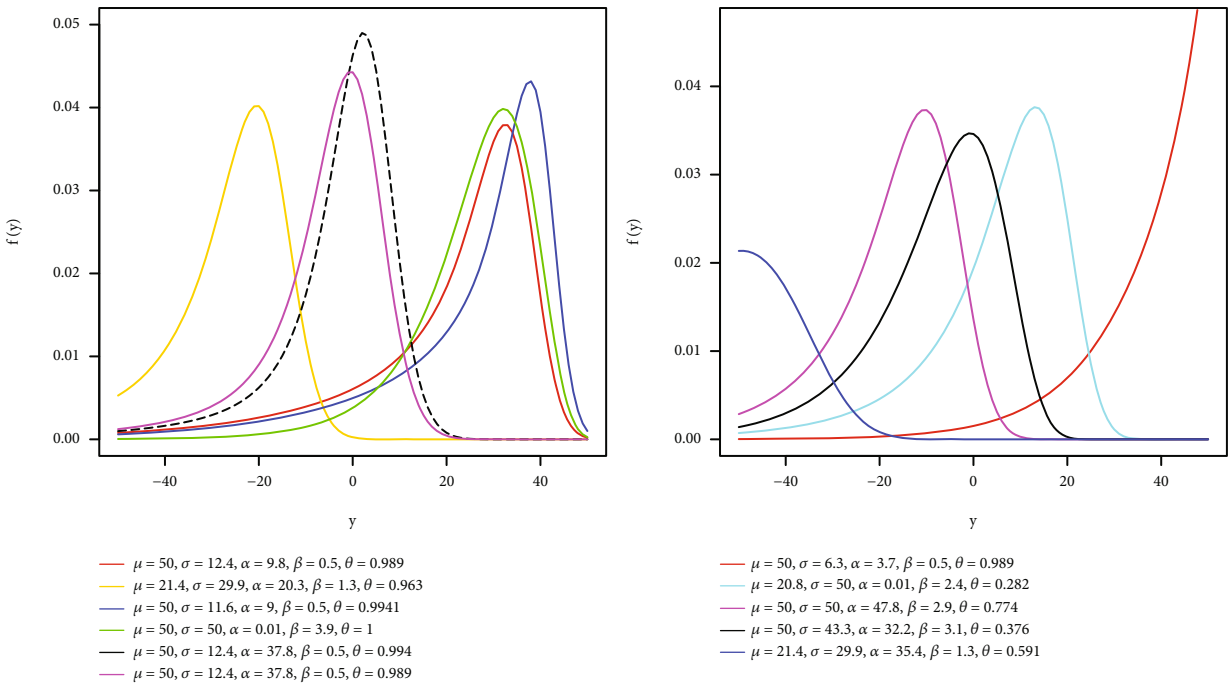

Figure 7: Density plot of the LHMWW distribution.

Table 1: Simulation results for HMWBIII distribution.

Parameter	n	I: (0.8, 0.3, 0.7, 0.5, 0.1)				II: (0.9, 0.2, 0.6, 0.5, 0.2)			
		AE	AB	RMSE	CP	AE	AB	RMSE	CP
a	25	1.8983	1.0983	2.3641	0.9750	2.0418	1.1418	2.4643	0.9750
	50	1.4282	0.6282	1.2945	0.9430	1.2953	0.3953	1.1303	0.9230
	100	1.0523	0.2523	0.7843	0.8910	1.0534	0.1534	0.5693	0.9070
	200	0.8651	0.0651	0.4136	0.9870	0.9442	0.0442	0.3715	0.8870
	300	0.8251	0.0251	0.3642	0.8960	0.9224	0.0224	0.2989	0.9100
	600	0.7961	−0.0039	0.2160	0.9730	0.9104	0.0204	0.2101	0.9480
b	25	0.3644	0.0644	0.3412	0.9610	0.2132	0.0132	0.1759	0.9040
	50	0.3163	0.0163	0.1211	0.9570	0.2021	0.0021	0.0746	0.9420
	100	0.3036	0.0036	0.0804	0.9700	0.1940	-0.0020	0.0479	0.9570
	200	0.2960	−0.0030	0.0591	0.9730	0.1947	-0.0017	0.0336	0.9680
	300	0.2936	−0.0026	0.0455	0.9710	0.1952	-0.0014	0.0291	0.9670
	600	0.2966	−0.0020	0.0336	0.9770	0.1955	-0.0010	0.0207	0.9720
α	25	1.3657	0.6657	4.6704	0.9500	1.0016	0.4016	3.6428	0.9530
	50	0.8532	0.1532	0.5086	0.9620	0.6866	0.0866	0.5260	0.9060
	100	0.7318	0.0318	0.3922	0.9760	0.5595	-0.0825	0.3987	0.9000
	200	0.6588	−0.0312	0.2796	0.9880	0.5168	-0.0802	0.3115	0.8950
	300	0.6438	−0.0304	0.2159	0.8980	0.5202	-0.0798	0.2803	0.9180
	600	0.6540	−0.0204	0.1551	0.9370	0.5154	-0.0646	0.2561	0.9640
β	25	0.3969	−0.1031	0.3037	0.8480	0.4180	-0.0820	0.2459	0.9850
	50	0.4407	−0.0593	0.2840	0.8700	0.4972	-0.0283	0.2477	0.9630
	100	0.5288	0.0294	0.2944	0.9740	0.5284	0.0284	0.2249	0.9160
	200	0.5606	0.0206	0.2634	0.9670	0.5427	0.0227	0.2027	0.8960
	300	0.5579	0.0179	0.2227	0.9060	0.5370	0.0170	0.1758	0.9550
	600	0.5384	0.0104	0.1632	0.9220	0.5107	0.0107	0.1106	0.9350
θ	25	0.1717	0.0717	0.0084	0.9560	0.1991	-0.0009	0.0078	0.9200
	50	0.1843	0.0843	0.0088	0.9420	0.2296	0.0296	0.0083	0.9860
	100	0.1673	0.0673	0.0081	0.9750	0.2219	0.0219	0.0078	0.9950
	200	0.1507	0.0507	0.0074	0.8730	0.2140	0.0140	0.0075	0.7870
	300	0.1371	0.0371	0.0066	0.7360	0.2110	0.0110	0.0071	0.8020
	600	0.1493	0.0493	0.0066	0.7640	0.2262	0.0262	0.0071	0.8090

where $x > 0$, $\alpha > 0$, $\beta > 0$, $0 < \theta < 1$, $a > 0$ and $b > 0$. The hazard function is given by

$$r(x) = \frac{\beta a b (1+ax)^{b\beta-1}\left[1-(1+ax)^{-b}\right]^{\beta-1}\left[\alpha(1-\theta)+\theta\exp\left\{-(\alpha-1)\left[(1+ax)^{b}-1\right]^{\beta}\right\}\right]}{1-\theta\left\{1-\exp\left[-(\alpha-1)\left((1+ax)^{b}-1\right)^{\beta}\right]\right\}}, x > 0. \quad (43)$$

The density function of HMWL distribution exhibited a wide variety shapes which include J-shape, reverse J-shape, right skewed, left skewed, and different forms of symmetric shapes as shown in Figure 2. The hazard rate function also exhibited varied shapes such as, upside down bathtub, monotone decreasing, and different forms of monotone increasing failure rates.

Table 2: Simulation results for HMWBIII distribution.

Parameter	n	III: (0.1, 0.3, 0.8, 1.2, 0.3)				IV: (0.9, 0.2, 0.5, 0.9, 0.1)			
		AE	AB	RMSE	CP	AE	AB	RMSE	CP
a	25	2.4464	1.4464	5.9733	0.9820	3.0165	2.1165	6.3116	0.9680
	50	2.0876	1.0876	4.1541	0.9660	1.8799	0.9799	3.2470	0.9320
	100	1.7410	0.7410	2.7987	0.9420	1.3400	0.4400	1.5736	0.8840
	200	1.4960	0.4960	2.1137	0.8900	1.0539	0.1539	0.6316	0.9860
	300	1.3042	0.3041	1.1947	0.8640	0.9674	0.0674	0.4545	0.8440
	600	1.0988	0.0988	0.7268	0.8200	0.9227	0.0227	0.3366	0.8440
b	25	0.4941	0.1941	0.9209	0.9820	0.2764	0.0764	0.8792	0.9700
	50	0.3591	0.0591	0.4413	0.9840	0.2123	0.0122	0.1056	0.9570
	100	0.3249	0.0249	0.1522	0.9850	0.2022	0.0022	0.0676	0.9620
	200	0.3380	0.0210	0.1270	0.9850	0.1988	−0.0012	0.0499	0.9660
	300	0.3386	0.0206	0.1090	0.9860	0.2011	0.0011	0.0440	0.9660
	600	0.3230	0.0130	0.1029	0.9810	0.1973	−0.0027	0.0337	0.9580
α	25	8.4405	7.6405	35.9691	0.8560	2.5174	2.0174	13.0567	0.9860
	50	3.6291	2.8291	19.3526	0.9060	0.8517	0.3517	0.9807	0.9570
	100	1.5109	0.7109	1.9017	0.8040	0.6049	0.1049	0.7391	0.9020
	200	1.5435	0.7035	1.8181	0.9770	0.5649	−0.0351	0.5147	0.8940
	300	1.4091	0.6091	1.6582	0.9470	0.4603	−0.0247	0.4125	0.7870
	600	1.2497	0.4497	1.5467	0.7410	0.4902	−0.0198	0.2668	0.8130
β	25	1.0983	−0.1017	1.4814	0.9740	0.7450	−0.1550	0.4456	0.9030
	50	1.1163	−0.0837	1.0444	0.9760	0.8046	−0.0954	0.4060	0.9190
	100	1.0757	−0.7843	0.5480	0.9720	0.8924	−0.0076	0.3739	0.9580
	200	1.2820	−0.0718	0.5940	0.9580	0.9329	0.0329	0.2883	0.9410
	300	1.1665	−0.0335	0.5549	0.9510	0.9276	0.0276	0.0265	0.9150
	600	1.2016	0.0016	0.4529	0.9080	0.9168	0.0268	0.2039	0.8810
θ	25	0.2493	−0.2507	0.0120	0.9040	0.1706	0.0706	0.0078	0.9770
	50	0.2592	−0.2408	0.0192	0.8270	0.1887	0.0887	0.0083	0.8180
	100	0.2953	−0.2047	0.0124	0.8230	0.2055	0.0755	0.0086	0.9720
	200	0.2961	−0.2039	0.0122	0.7680	0.1869	0.0729	0.0080	0.6440
	300	0.2768	−0.2032	0.0122	0.7230	0.1786	0.0686	0.0084	0.6430
	600	0.2903	−0.1097	0.0120	0.6770	0.1689	0.0682	0.0075	0.6150

The quantile function $Q_G(u)$ for the HMWL distribution is given by

$$(1-u)\left\{1-\theta\left[\exp\left(-(\alpha-1)\left((1+ax)^b-1\right)^\beta\right)\right]\right\} - \exp\left\{-\alpha\left[(1+ax)^b-1\right]^\beta\right\}=0. \tag{44}$$

5.3. Harmonic Mixture Weibull Weibull Distribution. Consider that the Weibull distribution is a baseline model with CDF and PDF, respectively, defined by Weibull [22] as $G(x)=1-e^{-ax^{-b}}$ and $g(x)=\mathrm{abx}^{b-1}e^{-ax^b}$, $x>0, a>0, b>0$. Then, the PDF of the Harmonic mixture Weibull Weibull (HMWW) distribution is given by

$$f(x)=\frac{\beta abx^{b-1}\left(1-e^{-ax^b}\right)^{\beta-1}\exp\left[\beta ax^b-\alpha\left(e^{ax^b}-1\right)^\beta\right]\left\{\alpha(1-\theta)+\theta\exp\left[-(\alpha-1)\left(e^{ax^b}-1\right)^\beta\right]\right\}}{\left\{1-\theta\left[1-\exp\left(-(\alpha-1)\left(e^{ax^b}-1\right)^\beta\right)\right]\right\}^2}, \tag{45}$$

Table 3: Ordered survival times of blood cancer patients.

115	461	807	1062	1251	1408	1578	1696
181	516	865	1063	1277	1455	1578	1735
255	739	924	1165	1290	1478	1599	1799
418	743	983	1181	1357	1222	1603	1815
441	789	1024	1222	1369	1549	1605	1852

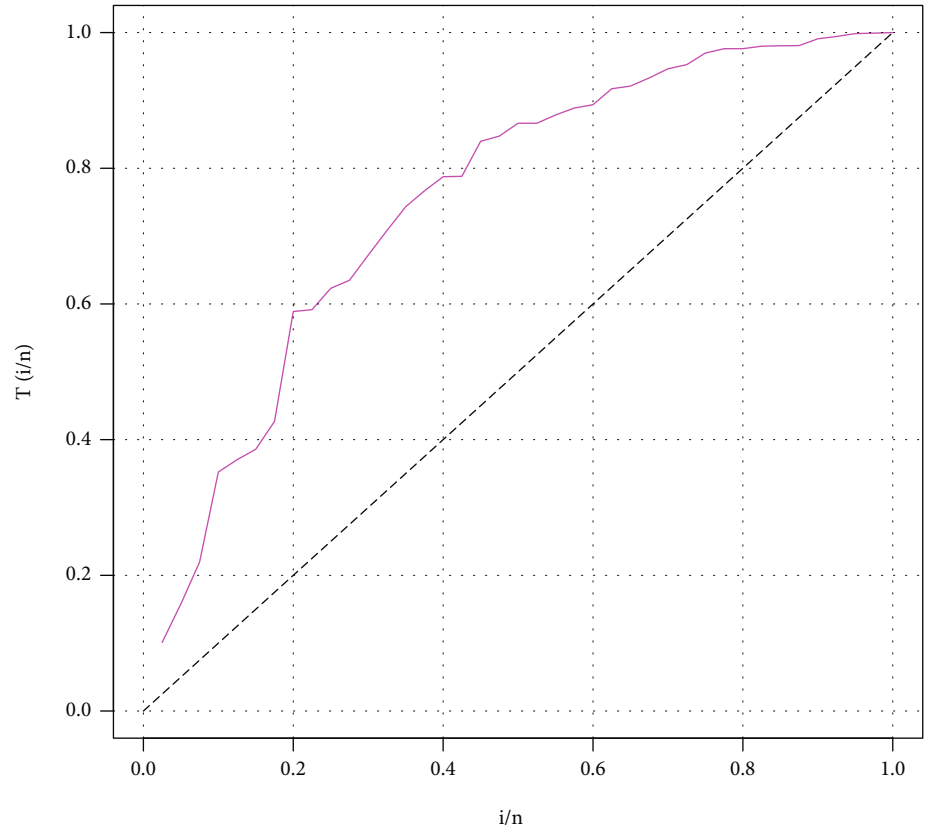

Figure 8: TTT plot for the blood cancer data.

where $x > 0, \alpha > 0, \beta > 0, 0 < \theta < 1, a > 0$ and $b > 0$. The hazard function is given by

$$r(x) = \frac{\beta a b x^{b-1} e^{\beta a x^b} \left(1 - e^{-a x^b}\right)^{\beta-1} \left\{\alpha(1-\theta) + \theta \exp\left[-(\alpha-1)\left(e^{a x^b} - 1\right)^{\beta}\right]\right\}}{1 - \theta\left\{1 - \exp\left[-(\alpha-1)\left(e^{a x^b} - 1\right)^{\beta}\right]\right\}}, x > 0. \tag{46}$$

The density plot of the HMWW distribution showed a wide variety of shapes such as; reverse *J*-shape, *J*-shape, right skewed, left skewed, and symmetric (with various levels of kurtosis) as shown in Figure 3. The hazard rate function also showed varying shapes such as, bathtub, upside-down bathtub, monotone decreasing, and various forms of monotone increasing failure rates for some selected parameter values.

The quantile function $Q_G(u)$ for the Harmonic mixture Weibull Weibull distribution is given by

$$(1-u)\left[1 - \theta\left\{\exp\left\{-(\alpha-1)\left[e^{a x^b} - 1\right]^{\beta}\right\}\right\}\right] - \exp\left\{-\alpha\left[e^{a x^b} - 1\right]^{\beta}\right\} = 0, u \in [0, 1]. \tag{47}$$

5.4. Harmonic Mixture Weibull Fréchet Distribution. Considering the Fréchet distribution as a baseline model with CDF and PDF, respectively, defined by Fréchet [23] as $G(x) = e^{-a x^{-b}}$ and $g(x) = a b x^{-b-1} e^{-a x^{-b}}, x > 0, a > 0, b > 0$, the PDF

Table 4: Parameter estimates of the fitted models on the blood cancer data.

Distribution	Parameter	Standard error	Z value	P value
HMWL	$\widehat{a} = 9.5631 \times 10^{1}$	2.9142×10^{-5}	3.2815×10^{6}	$<2.2000 \times 10^{-16***}$
	$\widehat{b} = 4.5590 \times 10^{-2}$	4.5879×10^{-4}	9.9371×10^{1}	$<2.2000 \times 10^{-16***}$
	$\widehat{\alpha} = 4.2570 \times 10^{2}$	6.2717×10^{-7}	6.7877×10^{8}	$<2.2000 \times 10^{-16***}$
	$\widehat{\beta} = 1.4647 \times 10^{1}$	2.2093×10^{-3}	6.6297×10^{3}	$<2.2000 \times 10^{-16***}$
	$\widehat{\theta} = 8.7947 \times 10^{-1}$	7.2549×10^{-2}	1.2122×10^{1}	$<2.2000 \times 10^{-16***}$
HMWW	$\widehat{a} = 1.8287 \times 10^{-2}$	1.2517×10^{-2}	1.4610	0.1440
	$\widehat{b} = 4.1880 \times 10^{-1}$	8.0455×10^{-2}	5.2054	$1.9360 \times 10^{-7***}$
	$\widehat{\alpha} = 40.9775$	3.0664×10^{-2}	1336.3478	$<2.2000 \times 10^{-16***}$
	$\widehat{\beta} = 3.3397$	1.5463	2.1598	$3.0790 \times 10^{-2*}$
	$\widehat{\theta} = 9.0063 \times 10^{-2}$	2.2115×10^{-1}	4.0725	$4.6510 \times 10^{-5***}$
GIW	$\widehat{\lambda} = 20.4052$	6.3882	3.1942	$1.4000 \times 10^{-3*}$
	$\widehat{\theta} = 1.1893$	0.1184	10.0464	$2.2000 \times 10^{-16***}$
	$\widehat{\mathrm{b}} = 69.0472$	1.5874	43.4970	$2.2000 \times 10^{-16***}$
OGEW	$\widehat{\alpha} = 2.7776$	1.0129	2.7422	$6.1020 \times 10^{-3**}$
	$\widehat{\beta} = 7.5292 \times 10^{-2}$	5.4895×10^{-2}	1.3716	0.1702
	$\widehat{\gamma} = 3.7906 \times 10^{-1}$	3.6964×10^{-2}	10.2548	$<2.0000 \times 10^{-16***}$
	$\widehat{\theta} = 2.1594 \times 10^{-1}$	5.3592×10^{-2}	4.0294	$5.5930 \times 10^{-5***}$
GOIEW	$\widehat{\alpha} = 1.7676$	0.5999	2.9467	$3.2000 \times 10^{-3*}$
	$\widehat{\beta} = 42.2469$	0.0143	2957.5338	$2.2000 \times 10^{-16***}$
	$\widehat{\gamma} = 0.0079$	0.0078	1.0162	0.3095
	$\widehat{\theta} = 0.8782$	0.1352	6.4966	$8.2140 \times 10^{-11***}$
GOIEL	$\widehat{\alpha} = 6.7875$	1.3537×10^{-1}	5.0139×10^{1}	$2.2000 \times 10^{-16***}$
	$\widehat{\beta} = 5.5062 \times 10^{2}$	6.6430×10^{-4}	8.2888×10^{5}	$2.2000 \times 10^{-16***}$
	$\widehat{\gamma} = 5.2442 \times 10^{-3}$	1.6279×10^{-3}	3.2213	$1.3000 \times 10^{-3*}$
	$\widehat{\theta} = 3.3683$	4.6765×10^{-1}	7.2026	$5.9070 \times 10^{-13***}$
E-lx	$\widehat{\alpha} = 2.0759 \times 10^{2}$	5.0510×10^{-5}	4.1099×10^{6}	$2.2000 \times 10^{-16***}$
	$\widehat{\lambda} = 1.0156 \times 10^{-1}$	4.7377×10^{-2}	2.1437	0.0321^{*}
	$\widehat{\theta} = 1.2399$	1.3932×10^{-1}	8.899	$2.2000 \times 10^{-16***}$

*means significant at 5% level of significance.

of the Harmonic mixture Weibull Fréchet (HMWF) distribution is given by

$$f(x) = \frac{\beta a b x^{-b-1} \exp\left\{-\left[\beta a x^{-b} + \alpha\left(e^{ax^{-b}} - 1\right)^{-\beta}\right]\right\}\left\{\alpha(1-\theta) + \theta \exp\left[-(\alpha-1)\left(e^{ax^{-b}} - 1\right)^{-\beta}\right]\right\}}{\left(1 - e^{-ax^{-b}}\right)^{\beta+1}\left\{1 - \theta\left[1 - \exp\left(-(\alpha-1)\left(e^{ax^{-b}} - 1\right)^{-\beta}\right)\right]\right\}^{2}}, \tag{48}$$

Table 5: Log-likelihood, goodness-of-fit statistics, and information criteria of the fitted models for the blood cancer data.

Model	ℓ	AIC	AICc	BIC	AD	CVM	K-S	*P* value
HMWL	-302.8800	615.7588	6007588	624.2032	0.6072	0.0627	0.0890	0.90950
HMWW	*-301.9300*	*613.8636*	*598.8636*	*622.3080*	*0.4728*	*0.0490*	*0.0859*	*0.9292*
GIW	-352.3200	710.6453	711.2607	715.9289	4.2362	0.7650	0.2607	0.0058
OGEW	-305.7900	619.5847	606.2514	626.3402	1.0067	0.1282	0.1320	0.4891
GOIEW	-330.4800	668.9273	669.9800	675.9721	1.5016	0.2553	0.1583	0.2687
GOIEL	-338.7500	685.5067	686.5593	692.5515	0.8518	0.1092	0.2477	0.0102
E-lx	-351.9400	709.8701	710.4855	715.1537	4.2210	0.7621	0.2520	0.0085

*bolded means best based on selection criteria.

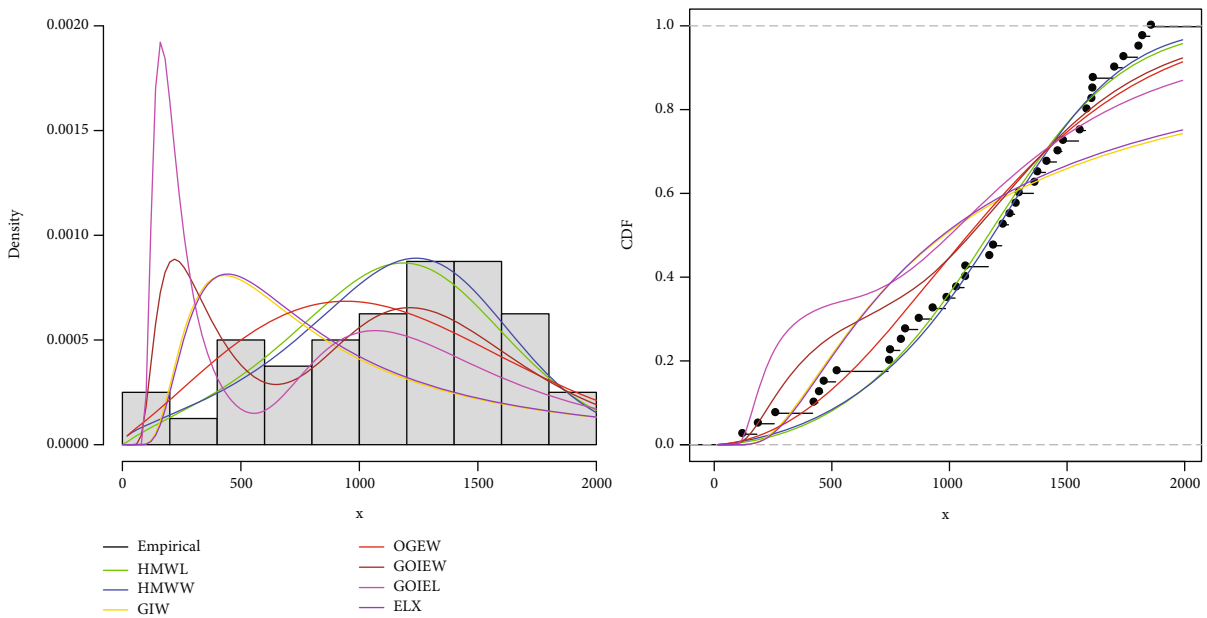

Figure 9: Fitted densities and CDFs plots of the blood cancer data.

Table 6: Survival times of diabetes patients.

52	18	69	19	28	74	25	29	56	39	76	26	81	33	34	38	38	34	35
43	45	45	63	47	46	42	42	42	41	46	45	45	43	41	40	49	49	48
53	53	35	54	61	54	55	55	25	73	51	74	37	56	58	58	58	57	50
18	62	62	81	63	47	64	64	65	67	60	36	68	19	69	61	61	61	70
75	83	52	62	33	80	26	76	75	37	29	39	51	35	59	50	82	52	52
71	51	73	24	51	48	48	40	54	36									

where $x > 0, \alpha > 0, \beta > 0, 0 < \theta < 1, a > 0$ and $b > 0$. The hazard function is given by

$$r(x) = \frac{\beta a b x^{-b-1} e^{-\beta a x^{-b}} \left\{ \alpha(1-\theta) + \theta \exp\left[-(\alpha-1)\left(e^{a x^{-b}} - 1\right)^{-\beta} \right] \right\}}{\left(1 - e^{-a x^{-b}}\right)^{\beta+1} \left\{ 1 - \theta \left[1 - \exp\left(-(\alpha-1)\left(e^{a x^{-b}} - 1\right)^{-\beta} \right) \right] \right\}}, x > 0. \tag{49}$$

The density plot of the HMWF distribution exhibited a wide variety of attractive shapes such as, *J*-shape, reverse *J*-shape, right skewed, left skewed, and various forms of symmetric shapes as shown in Figure 4. The hazard rate function also showed varying shapes such as; upside-down bathtub, monotone decreasing and different forms of monotone increasing failure rates for some selected parameter values.

The quantile function $Q_G(u)$ for the Harmonic mixture Weibull Fréchet distribution is given by

$$(1-u)\left\{ 1 - \theta \left[\exp\left(-(\alpha-1)\left(e^{a x^{-b}} - 1\right)^{-\beta} \right) \right] \right\} - \exp\left[-\alpha \left(e^{a x^{-b}} - 1\right)^{-\beta} \right] = 0, u \in [0,1] \tag{50}$$

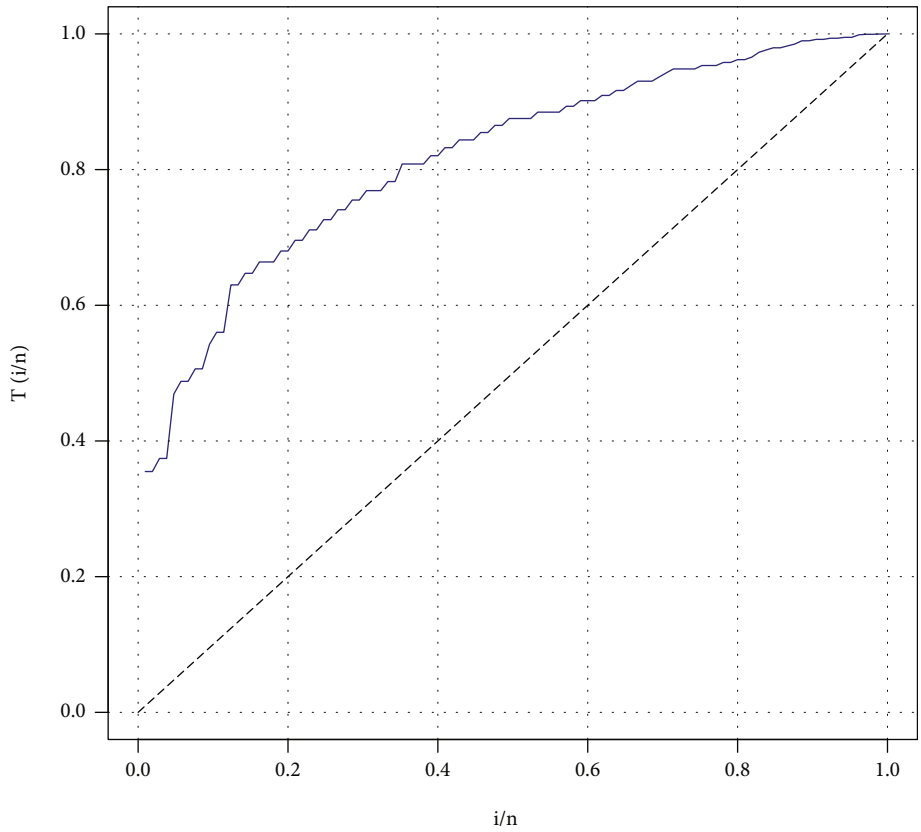

Figure 10: TTT plot for the diabetes data.

5.5. Harmonic Mixture Weibull Normal Distribution. Consider that the Normal distribution is a baseline model with the CDF and PDF, respectively, given by $G(x) = \Phi((x-\mu)/\sigma)$ and $g(x) = 1/(\sigma\sqrt{2\pi})e^{-1/2((x-\mu)/\sigma)^2}$, $-\infty < x < \infty$, $-\infty < \mu < \infty$, $\sigma > 0$. Then, the PDF of the Harmonic mixture Weibull Normal (HMWN) distribution is given by

$$f(x) = \beta\left[\Phi\left(\frac{x-\mu}{\sigma}\right)\right]^{\beta-1} \exp\left\{-\left[\frac{1}{2}\left(\frac{x-\mu}{\sigma}\right)^2 + \alpha\left(\left(\Phi\left(\frac{x-\mu}{\sigma}\right)\right)^{-1} - 1\right)^{-\beta}\right]\right\} \times \frac{\alpha(1-\theta) + \theta \exp\left\{-(\alpha-1)\left[(\Phi((x-\mu)/\sigma))^{-1} - 1\right]^{-\beta}\right\}}{\sigma\sqrt{2\pi}[1-\Phi((x-\mu)/\sigma)]^{\beta+1}\left\{1-\theta\left[1-\exp\left(-(\alpha-1)\left((\Phi((x-\mu)/\sigma))^{-1}-1\right)^{-\beta}\right)\right]\right\}^2}, \tag{51}$$

where $-\infty < x < \infty, \alpha > 0, \beta > 0, 0 < \theta < 1, -\infty < \mu < \infty$ and $\sigma > 0$.
The hazard function is given by

$$r(x) = \frac{\beta e^{-1/2((x-\mu)/\sigma)^2}[\Phi((x-\mu)/\sigma)]^{\beta-1}\left\{\alpha(1-\theta) + \theta \exp\left[-(\alpha-1)\left((\Phi((x-\mu)/\sigma))^{-1}-1\right)^{-\beta}\right]\right\}}{\sigma\sqrt{2\pi}[1-\Phi((x-\mu)/\sigma)]^{\beta+1}\left\{1-\theta\left[1-\exp\left(-(\alpha-1)\left((\Phi((x-\mu)/\sigma))^{-1}-1\right)^{-\beta}\right)\right]\right\}}, -\infty < x < \infty. \tag{52}$$

Table 7: Parameter estimates of the fitted models on the diabetes data.

Distribution	Parameter estimate	Standard error	Z value	P value
HMWL	$\widehat{a} = 3.7238 \times 10^{-3}$	1.3636×10^{-3}	2.7308	$6.3170 \times 10^{-3**}$
	$\widehat{b} = 2.2400$	7.0116×10^{-1}	3.1947	$1.4000 \times 10^{-3**}$
	$\widehat{\alpha} = 7.3882$	2.7030×10^{-2}	273.3389	$<2.2000 \times 10^{-16***}$
	$\widehat{\beta} = 3.1315$	1.5959×10^{-1}	19.6221	$<2.2000 \times 10^{-16***}$
	$\widehat{\theta} = 8.5928 \times 10^{-2}$	1.6698×10^{-1}	0.5146	0.6068
HMWW	$\widehat{a} = 3.2731 \times 10^{-1}$	3.5914×10^{-2}	9.1137	$<2.2000 \times 10^{-16***}$
	$\widehat{b} = 1.3193 \times 10^{-1}$	2.3472×10^{-2}	5.6205	$1.9050 \times 10^{-8***}$
	$\widehat{\alpha} = 4.3077 \times 10^{2}$	2.0874×10^{-5}	2.0637×10^{7}	$<2.2000 \times 10^{-16***}$
	$\widehat{\beta} = 2.0680 \times 10^{1}$	1.0524×10^{-2}	1.9651×10^{3}	$<2.2000 \times 10^{-16***}$
	$\widehat{\theta} = 3.3286 \times 10^{-3}$	7.2963×10^{-1}	4.6000×10^{-3}	0.9964
GIW	$\widehat{\lambda} = 14.3949$	7.8816×10^{-1}	18.2640	$<2.2000 \times 10^{-16***}$
	$\widehat{\theta} = 2.4880$	1.6693×10^{-1}	14.9040	$<2.2000 \times 10^{-16***}$
	$\widehat{b} = 12.4789$	3.6543×10^{-1}	34.1490	$<2.2000 \times 10^{-16***}$
OGEW	$\widehat{\alpha} = 6.2007$	1.0197×10^{-2}	608.0858	$<2.0000 \times 10^{-16***}$
	$\widehat{\beta} = 6.2572$	3.4785×10^{-3}	1798.8481	$<2.0000 \times 10^{-16***}$
	$\widehat{\gamma} = 1.1785$	9.7083×10^{-2}	12.1387	$<2.0000 \times 10^{-16***}$
	$\widehat{\theta} = 3.1583 \times 10^{-3}$	1.2296×10^{-3}	2.5686	$1.0210 \times 10^{-2*}$
GOIEW	$\widehat{\alpha} = 3.8264$	9.3022×10^{-1}	4.1134	$3.8990 \times 10^{-5***}$
	$\widehat{\beta} = 45.7623$	5.6602×10^{-2}	808.4855	$<2.2000 \times 10^{-16***}$
	$\widehat{\gamma} = 2.7834 \times 10^{-2}$	1.6309×10^{-2}	1.7067	0.0879
	$\widehat{\theta} = 1.2618$	1.4195×10^{-1}	8.8889	$<2.2000 \times 10^{-16***}$
GOIEL	$\widehat{\alpha} = 1.1535 \times 10^{1}$	1.3294	8.6765	$<2.2000 \times 10^{-16***}$
	$\widehat{\beta} = 9.9124 \times 10^{1}$	7.1690×10^{-2}	1382.6765	$<2.2000 \times 10^{-16***}$
	$\widehat{\gamma} = 1.1493 \times 10^{-2}$	6.3054×10^{-4}	18.2274	$<2.2000 \times 10^{-16***}$
	$\widehat{\theta} = 1.0812 \times 10^{1}$	5.0939×10^{-1}	21.2258	$<2.2000 \times 10^{-16***}$
E-lx	$\widehat{\alpha} = 1.7112 \times 10^{1}$	4.3906×10^{-8}	3.8975×10^{8}	$<2.2000 \times 10^{-16***}$
	$\widehat{\lambda} = 7.1402 \times 10^{-3}$	2.8425×10^{-4}	2.5119×10^{1}	$<2.2000 \times 10^{-16***}$
	$\widehat{\theta} = 1.1041 \times 10^{1}$	2.1284×10^{-7}	5.1872×10^{7}	$<2.2000 \times 10^{-16***}$

*means significant at 5% level of significance.

Table 8: Log-likelihood, goodness-of-fit statistics, and information criteria for the Diabetes data.

Model	ℓ	AIC	AICc	BIC	AD	CVM	K-S	P value
HMWL	-438.8100	887.6210	872.6210	900.8908	0.2264	0.0283	0.0431	0.9899
HMWW	*-438.7500*	*887.5028*	*872.5028*	*900.7726*	*0.2075*	*0.0222*	*0.0424*	*0.9916*
GIW	-464.7700	935.5496	923.5496	943.5114	4.3892	0.6870	0.1476	0.0207
OGEW	-441.7500	891.5075	878.1742	902.1234	0.6742	0.1044	0.0728	0.6342
GOIEW	-442.3900	892.7726	879.4393	903.3885	1.2195	0.1885	0.1111	0.1500
GOIEL	-447.9600	903.9159	890.5826	914.5317	3.1652	0.5774	0.1392	0.0342
E-lx	-449.8500	905.6986	893.6986	913.6605	1.9525	0.2891	0.1028	0.2174

*bolded means best based on selection criteria.

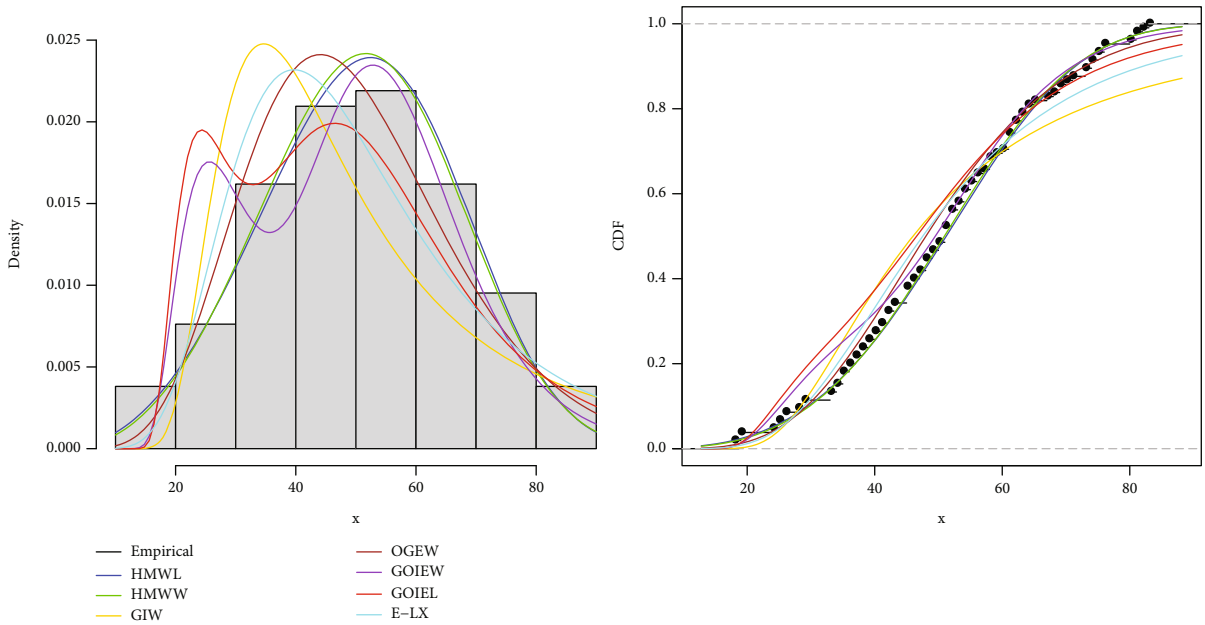

Figure 11: Plots of fitted densities and CDFs of the diabetes data.

Table 9: Survival times of hypertension patients.

71	5	39	62	52	71	38	56	35	69	34	71	66
70	52	37	35	71	73	19	74	74	75	51	76	49
19	76	78	76	76	49	47	48	48	46	46	46	41
40	43	45	47	47	44	45	46	42	43	42	20	28
26	60	27	24	29	60	25	60	69	36	69	69	68
68	67	67	67	52	35	66	55	66	61	61	64	64
65	65	63	63	62	39	62	62	62	59	59	59	58
58	58	18	57	57	56	56	37	53	53	53	53	54
54	66	17	50	75	51	38	52	66	4	52	55	19
58	73											

The density plot of the HMWN distribution exhibited a very wide variety of attractive shapes such as unimodal right skewed, unimodal left skewed, symmetric (with different levels of kurtosis), *J*-shape, reverse *J*-shape, bimodal (with different levels of kurtosis), bimodal left skewed, and *N*-shapes as shown in Figure 5. The hazard rate function also showed a wide variety of very flexible shapes such as, bathtub, upside-down bathtub, various forms of modified upside-down bathtubs, monotone decreasing, and different forms of monotone increasing failure rates for some selected values as shown in Figure 6.

The quantile function $Q_G(u)$ for the Harmonic mixture Weibull Normal distribution is given by

$$(1-u)\left\{1-\theta\left[\exp\left(-(\alpha-1)\left(\left(\Phi\left(\frac{x-\mu}{\sigma}\right)\right)^{-1}-1\right)^{-\beta}\right)\right]\right\} - \exp\left\{-\alpha\left[\left(\Phi\left(\frac{x-\mu}{\sigma}\right)\right)^{-1}-1\right]^{-\beta}\right\} = 0,\ u\in[0,1]. \tag{53}$$

6. Log-HMWW Location-Scale Regression

In this section, the log-HMWW regression model is presented. Suppose the random variable X follows the HMWW distribution, then $Y=\log(X)$ follows the log Harmonic mixture Weibull Weibull (LHMWW) distribution. Let $a=e^{-\mu/\sigma}$ and $b=1/\sigma$. Following the given reparameterization, the density function of the LHMWW distribution is

$$f_y(y)=\frac{\beta}{\sigma}\exp\left(\frac{y-\mu}{\sigma}\right)\left\{1-\exp\left[-\exp\left(\frac{y-\mu}{\sigma}\right)\right]\right\}^{\beta-1}\exp \cdot\left\{\beta\exp\left(\frac{y-\mu}{\sigma}\right)-\alpha\left[\exp\left(\exp\left(\frac{y-\mu}{\sigma}\right)\right)-1\right]^{\beta}\right\} \times\frac{\left\{\alpha(1-\theta)+\theta\exp\left[-(\alpha-1)(\exp(\exp((x-\mu)/\sigma))-1)^{\beta}\right]\right\}}{\left\{1-\theta\left[1-\exp\left(-(\alpha-1)(\exp(\exp((x-\mu)/\sigma))-1)^{\beta}\right)\right]\right\}^{2}},\ y\in\mathbb{R}, \tag{54}$$

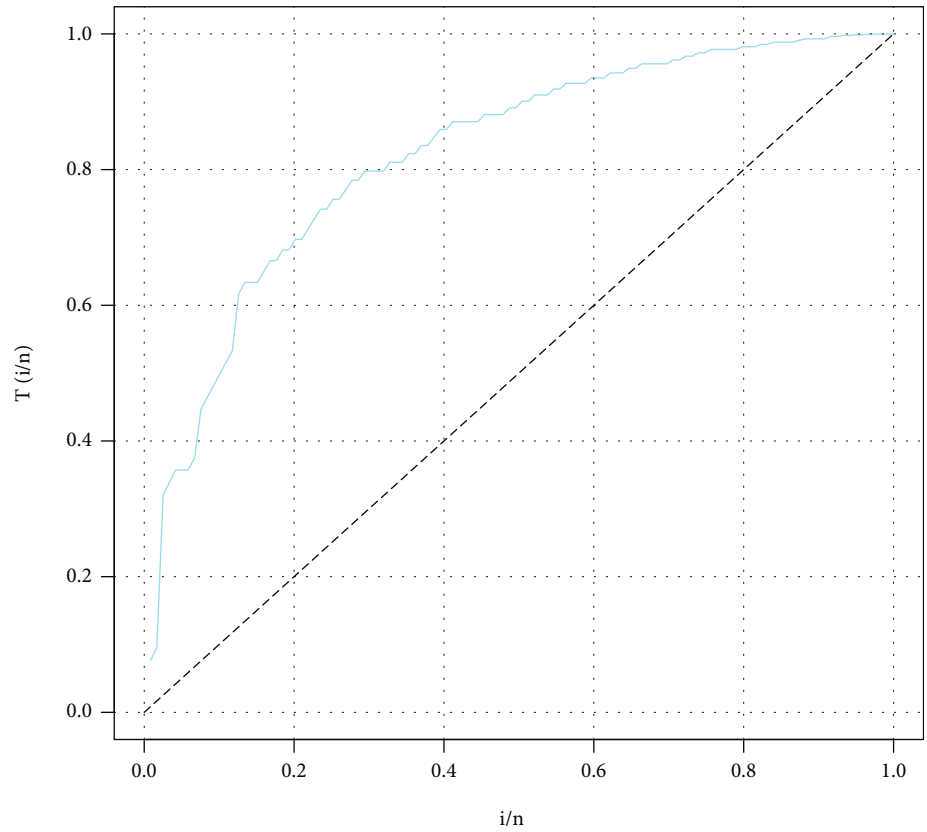

Figure 12: TTT plot for the hypertension data.

where $-\infty < \mu < \infty$ is the location parameter, $\sigma > 0$, $\alpha > 0$ and $0 < \theta < 1$ are the scale parameters and $\beta > 0$ is the shape parameter. The density plot of the LHMWW distribution exhibited varying shapes such as, *J*-shape, reverse *J*-shape, right skewed, symmetric, and left skewed shapes as shown in Figure 7. By these properties, the LHMWW distribution is capable of modelling right skewed, symmetric and left skewed dependent variable with covariates in medical studies.

The corresponding survival function to (54) is given by

$$S(y;\alpha,\beta,\sigma,\mu) = \frac{\exp\left\{-\alpha[\exp(\exp((x-\mu)/\sigma))-1]^{\beta}\right\}}{1-\theta\left\{1-\exp\left[-(\alpha-1)(\exp(\exp((x-\mu)/\sigma))-1)^{\beta}\right]\right\}}, \mathrm{y} \in \mathbb{R}. \tag{55}$$

Suppose that $z = (y-\mu)/\sigma$ is the standardized random variable, then the PDF is written as

$$\begin{aligned} f_y(y) = {} & \frac{\beta}{\sigma}\exp(z)\{1-\exp[-\exp(z)]\}^{\beta-1}\exp \\ & \cdot\left\{\beta\exp(z)-\alpha[\exp(\exp(z))-1]^{\beta}\right\} \\ & \times\frac{\alpha(1-\theta)+\theta\exp\left\{-(\alpha-1)[\exp(\exp(z))-1]^{\beta}\right\}}{\left\{1-\theta\left[1-\exp\left(-(\alpha-1)(\exp(\exp(z))-1)^{\beta}\right)\right]\right\}^{2}}, \mathrm{y} \in \mathbb{R}. \end{aligned} \tag{56}$$

By using the LHMWW density, we develop the LHMWW location-scale regression model with the following regression structure

$$y_j = \mathbf{v}_j^T\boldsymbol{\gamma} + \sigma z_j, i = 1, 2, \cdots, n, \tag{57}$$

where $\mu = \mathbf{v}_j^T\gamma$ is the location parameter which depends on a particular set of covariates, $\boldsymbol{\gamma} = (\gamma_1, \gamma_2, \cdots, \gamma_k)^T$ is a $k \times 1$ parameter vector for the regression model, $\mathbf{v}_j = (v_{j1}, v_{j2}, \cdots, v_{jk})^T$ is the set of covariates, and z_j is the error term that follows the LHMWW distribution. The unknown parameters of the LHMWW regression model are estimated using the maximum likelihood estimation procedure. The log-likelihood function of the LHMWW regression model is given by

$$\begin{aligned} \ell = {} & n\log\left(\frac{\beta}{\sigma}\right) + \sum_{j=1}^{n} z_j + (\beta-1)\sum_{j=1}^{n}\{1-\exp[-\exp(z_j)]\} \\ & + \sum_{j=1}^{n}\left\{\beta\exp(z_j) - \alpha[\exp(\exp(z_j))-1]^{\beta}\right\} \\ & + \sum_{j=1}^{n}\log\left\{\alpha(1-\theta)+\theta\exp\left[-(\alpha-1)(\exp(\exp(z_j))-1)^{\beta}\right]\right\} \\ & - 2\sum_{j=1}^{n}\log\left\{1-\theta\left[1-\exp\left(-(\alpha-1)(\exp(\exp(z_j))-1)^{\beta}\right)\right]\right\}, \end{aligned} \tag{58}$$

where $z_j = (y_j - \mathbf{v}_j^T\boldsymbol{\gamma})/\sigma$ and n is the number of observations.

Table 10: Parameter estimates of the fitted models on the hypertension data.

Distribution	Parameter estimate	Standard error	Z-value	P value
HMWL	$\widehat{a} = 3.0825 \times 10^{-3}$	2.4265×10^{-4}	12.7035	$<2.2000 \times 10^{-16***}$
	$\widehat{b} = 4.3675$	1.0806×10^{-1}	40.4177	$<2.2000 \times 10^{-16***}$
	$\widehat{\alpha} = 1.0912 \times 10^{-1}$	1.5700×10^{-1}	0.6950	0.4871
	$\widehat{\beta} = 2.9417$	3.0333×10^{-1}	9.6981	$<2.2000 \times 10^{-16***}$
	$\widehat{\theta} = 6.2795 \times 10^{-1}$	2.0319×10^{-1}	3.0905	$1.9980 \times 10^{-3**}$
HMWW	$\widehat{a} = 1.2373 \times 10^{-1}$	4.9012×10^{-2}	2.5244	0.0116^{*}
	$\widehat{b} = 2.9675 \times 10^{-1}$	6.8779×10^{-2}	4.3146	$1.5990 \times 10^{-5***}$
	$\widehat{\alpha} = 2.0787 \times 10^{2}$	3.6742×10^{-3}	56575.9248	$<2.2000 \times 10^{-16***}$
	$\widehat{\beta} = 6.4744$	1.8346	3.5290	$4.1710 \times 10^{-4***}$
	$\widehat{\theta} = 8.9463 \times 10^{-1}$	9.1076×10^{-2}	9.8230	$<2.2000 \times 10^{-16***}$
GIW	$\widehat{\lambda} = 3.9662 \times 10^{-1}$	9.0450×10^{-2}	4.3850	$1.1600 \times 10^{-5***}$
	$\widehat{\theta} = 1.3075$	7.0211×10^{-2}	1.8622×10^{1}	$<2.2000 \times 10^{-16***}$
	$\widehat{b} = 3.7129 \times 10^{2}$	7.3899×10^{-5}	5.0244×10^{6}	$<2.2000 \times 10^{-16***}$
OGEW	$\widehat{\alpha} = 2.1588$	1.1590×10^{-1}	18.6271	$<2.0000 \times 10^{-16***}$
	$\widehat{\beta} = 6.5927 \times 10^{-1}$	2.5204×10^{-1}	2.6157	$8.9030 \times 10^{-3**}$
	$\widehat{\gamma} = 1.5725$	1.7709×10^{-1}	8.8798	$<2.0000 \times 10^{-16***}$
	$\widehat{\theta} = 2.0899 \times 10^{-3}$	1.9202×10^{-3}	1.0884	0.2764
GOIEW	$\widehat{\alpha} = 6.0373 \times 10^{-1}$	1.1470×10^{-1}	5.2634	$1.4140 \times 10^{-7***}$
	$\widehat{\beta} = 13.6055$	1.1507×10^{-2}	1182.3470	$<2.2000 \times 10^{-16***}$
	$\widehat{\gamma} = 4.5046 \times 10^{-3}$	3.6406×10^{-3}	1.2373	0.2160
	$\widehat{\theta} = 1.6297$	1.9507×10^{-1}	8.3542	$<2.2000 \times 10^{-16***}$
GOIEL	$\widehat{\alpha} = 1.9042$	2.6522×10^{-1}	7.1796	$6.9910 \times 10^{-13***}$
	$\widehat{\beta} = 9.8331 \times 10^{1}$	9.2359×10^{-4}	1.0647×10^{5}	$<2.2000 \times 10^{-16***}$
	$\widehat{\gamma} = 8.7185 \times 10^{-3}$	2.6638×10^{-4}	3.2729×10^{1}	$<2.2000 \times 10^{-16***}$
	$\widehat{\theta} = 1.3273 \times 10^{1}$	5.1568×10^{-3}	2.5739×10^{3}	$<2.2000 \times 10^{-16***}$
E-lx	$\widehat{\alpha} = 7.0654$	1.1455	6.1680	$6.9150 \times 10^{-10***}$
	$\widehat{\lambda} = 3.8023 \times 10^{-3}$	2.9418×10^{-4}	12.9250	$<2.2000 \times 10^{-16***}$
	$\widehat{\theta} = 1.4008 \times 10$	8.3986×10^{-2}	166.7850	$<2.2000 \times 10^{-16***}$

*means significant at 5% significance level.

By maximizing the log-likelihood function in (58), the parameter estimates of the LHMWW regression model are obtained. The adequacy of the regression model is evaluated by using the Cox-Snell residuals [24]. The Cox-Snell residuals of the LHMWW regression model are given by $r_j = -\log(S(y_j|\alpha, \beta, \sigma, \mu)), j = 1, 2, \cdots, n,$ where $S(y_j|\alpha, \beta, \sigma, \mu)$ is defined as in (55). The Cox-Snell residuals plots are expected to follow the standard exponential distribution if the LHMWW regression model gives a good fit to a data set.

7. Simulation

In this section, the finite sample properties of the maximum likelihood estimators of the parameters are investigated using Monte Carlo simulations. The Monte Carlo simulations were performed by using the estimators of the HMWBIII distribution. The quantile function of the HMWBIII distribution was used to generate random samples from the HMWBIII distribution. The simulation experiment was replicated 1000 times for each of the sample sizes $n = 25$, 50, 100, 200, 300, and

Table 11: Log-likelihood, goodness-of-fit statistics, and information criteria of the fitted models for hypertension data.

Model	ℓ	AIC	AICc	BIC	AD	CVM	K-S	P value
HMWL	−497.9700	1005.9490	990.9490	1019.8450	0.8176	0.0485	0.0536	0.8834
HMWW	*-496.4200*	*1002.8500*	*987.8500*	*1016.7460*	*0.6299*	*0.0575*	*0.0509*	*0.9170*
GIW	−592.6100	1191.2200	1179.2200	1199.5570	15.9110	2.9605	0.3111	1.974×10^{-10}
OGEW	−499.6900	1007.3730	994.0397	1018.4900	1.1156	0.1211	0.0656	0.6847
GOIEW	−513.0200	1034.0340	1020.7010	1045.1510	8.1430	1.5363	0.1966	0.0002
GOIEL	−531.9800	1071.9600	1058.6270	1083.0770	14.0020	2.7726	0.2431	1.5620×10^{-6}
E-lx	−538.1700	1078.3340	1066.3340	1086.6710	7.3446	1.2976	0.1767	0.0012

*bolded means best based on selection criteria.

600 with parameter values $(a, b, \alpha, \beta, \theta)$ = I: (0.8, 0.3, 0.7, 0.5, 0.1), II: (0.9, 0.2, 0.6, 0.5, 0.2), III: (0.1, 0.3, 0.8, 1.2, 0.3), and IV: (0.9, 0.2, 0.5, 0.9, 0.1). The average estimate (AE), the average bias (AB), the root mean square error (RMSE), and the coverage probability (CP) were used to assess the performance of the estimators of the parameters. Generally, the AE values converge to the actual parameter values as the sample size increases and the RMSE also decreases as the sample size increases. The AB values also converge to zero (0) with increase in the sample size as shown in Table 1 and Table 2. The CP values for most of the estimators are also observed to revolve around the nominal value of 0.975. These characteristics demonstrate that the maximum likelihood method works very effectively in estimating the parameters of the developed family. It also shows that the estimators of the developed family are asymptotically consistent, efficient and unbiased.

8. Applications of the HMW-G Family

The applications of the special distributions (HMWL and HMWW) of the HMW-G family to real data sets in medical studies are illustrated in this section. To this end, the special distributions of the family are fitted to real data sets and their performances compared to other competing distributions including generalized inverse Weibull (GIW) distribution [25], odd generalized exponential Weibull (OGEW) distribution [26], generalized odd inverse exponential Weibull (GOIEW), and generalized odd inverse exponential Lomax (GOIEL) distributions [27, 28], and exponentiated Lomax (E-Lx) distribution [29]. The total time on test (TTT) plot due to Aarset [30] is used in assessing the applicability of the special distributions to the real data sets. Goodness of fit tests such as Anderson-Darling (AD) test, Cramér-von Mises (CVM) test, and Kolmogorov-Smirnov (K-S) test as well as Akaike information criterion (AIC), corrected AIC (AICc), Bayesian information criterion (BIC), and the log-likelihood are used to assess the performances of the fitted distributions. The P values of the K-S test are provided. A model with the least values of the goodness of fit measures and highest value of the log-likelihood represents the best fitted model for the data set.

8.1. First Application. The first data set represents the ordered survival times of blood cancer patients. The data is found in Abouammoh et al. [31]. It can also be found in Amadu [27] and Amadu et al. [28]. The ordered survival times for 40 patients are given in Table 3.

The TTT plot in Figure 8 indicates that the blood cancer data exhibit an increasing failure rate and hence, the HMW-G family is appropriate to fit the data set.

In Table 4, the maximum likelihood parameter estimates of the fitted distributions is presented.

Table 5 presents the goodness of fit measures of the fitted distributions on the blood cancer data. The results generally show that the HMWW and HMWL distributions provide better fits to the blood cancer data than the other competing models with the HMWW distribution being the overall best fitted model.

Figure 9 shows the densities and CDFs plots of the fitted models. The results give a confirmation that the HMWW distribution provides a better fit to the data than the other competing models.

8.2. Second Application. The second data set represents the survival times (life lengths in years) until onset of diabetes from a random sample of 105 patients obtained from the Bolgatanga Regional Hospital in the Upper East region of Ghana. The data set is shown in Table 6.

The TTT plot in Figure 10 indicates that the diabetes data exhibit an increasing failure rate and hence, the HMW-G family is appropriate to fit the data set.

In Table 7, the maximum likelihood estimates of the parameters of the fitted distributions are presented.

Table 8 presents the goodness of fit measures of the fitted models. The results show that the special distributions (HMWW and HMWL) of the HMW-G family generally provide better fits to the diabetes data than the other competing models with the HMWW distribution being the overall best fitted model.

Figure 11 shows the densities and CDFs plots of the fitted models. The results confirm that the HMWW and HMWL distributions of the HMW-G family generally provide better fits to the data than the other competing models.

8.3. Third Application. The third data set represents the survival times (life lengths in years) until onset of hypertension from a random sample of 119 patients obtained from the Bolgatanga Regional Hospital in the Upper East region of Ghana. The data set is shown in Table 9.

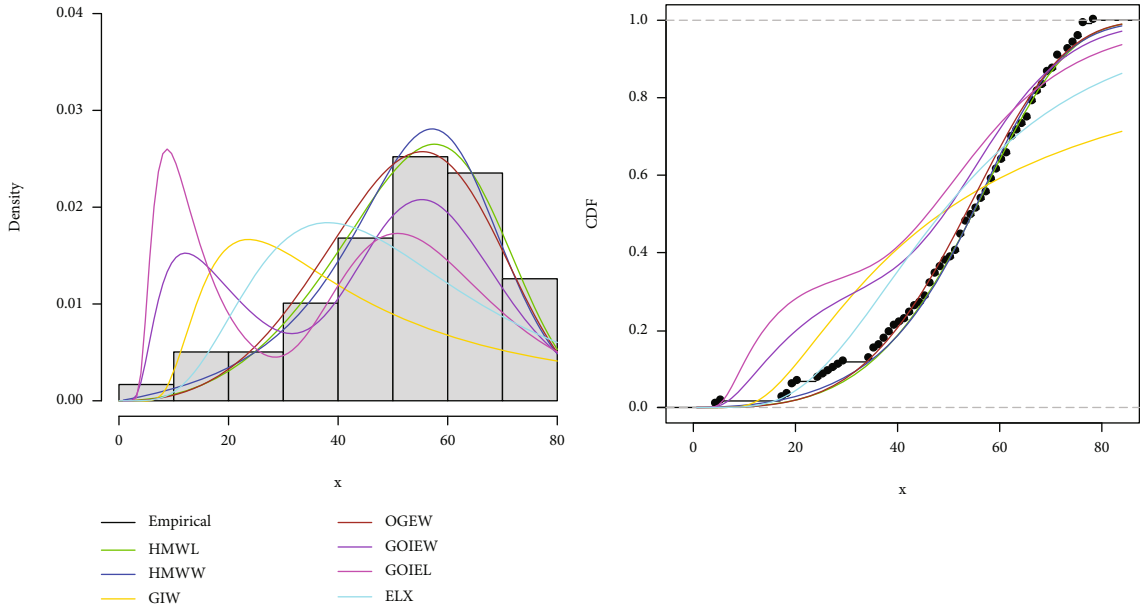

Figure 13: Plots of fitted densities and CDFs of the hypertension data.

Table 12: Hypertension data with covariate (gender).

71(1)	5(1)	39(1)	62(1)	52(0)	71(0)	38(0)	56(1)	35(1)	69(1)	34(1)	71(1)	66(0)
70(1)	52(0)	37(0)	35(0)	71(1)	73(1)	19(0)	74(0)	74(1)	75(1)	51(0)	76(1)	49(0)
19(1)	76(0)	78(1)	76(0)	76(0)	49(1)	47(1)	48(0)	48(0)	46(0)	46(1)	46(1)	41(0)
40(0)	43(1)	45(0)	47(0)	47(0)	44(0)	45(1)	46(1)	42(1)	43(0)	42(0)	20(1)	28(0)
26(0)	60(0)	27(1)	24(0)	29(0)	60(1)	25(1)	60(1)	69(1)	36(1)	69(0)	69(1)	68(0)
68(0)	67(1)	67(0)	67(0)	52(0)	35(0)	66(0)	55(0)	66(1)	61(1)	61(0)	64(0)	64(0)
65(0)	65(0)	63(1)	63(1)	62(0)	39(1)	62(0)	62(0)	62(0)	59(1)	59(0)	59(1)	58(0)
58(0)	58(0)	18(1)	57(0)	57(0)	56(0)	56(0)	37(1)	53(0)	53(0)	53(0)	53(1)	54(1)
54(1)	66(0)	17(0)	50(0)	75(0)	51(0)	38(0)	52(1)	66(0)	4(1)	52(0)	55(0)	19(1)
58(1)	73(0)											

The TTT plot in Figure 12 indicates that the hypertension data exhibit an increasing failure rate and therefore, the HMW-G family is appropriate to fit the data set.

Table 10 shows the maximum likelihood estimates of the parameters of the fitted distributions.

The goodness of fit measures of the fitted models on the hypertension data are given in Table 11. The results show that the HMWW and HMWL distributions of the HMW-G family generally provide better fits to the data than the other competing models with the HMWW distribution being the overall best fitted model.

The densities and CDFs plots of the fitted models are shown in Figure 13. The results give a confirmation that the HMWW distribution provides a better fit to the data than the other competing models.

8.4. Fourth Application. In this section, the application of the LHMWW location-scale regression model is demonstrated by modelling a real data set. The data set obtained from the Bolgatanga Regional Hospital in the Upper East Region of Ghana represents the survival times (life lengths in years) until onset of hypertension from a random sample of 119 patients with gender as a covariate. The gender (1 = male, 0 = female) is presented in brackets for each survival time. The data set is given in Table 12.

The dependent variable, time until the onset of hypertension y_j, is modelled with gender x_{j1} (1 = male, 0 = female) as the covariate. To this end, the following regression model is fitted to the data set

$$y_j = \gamma_0 + \gamma_1 v_{j1} + \sigma z_j, \tag{59}$$

where y_j follows the LHMWW distribution. The performance of the LHMWW regression model was assessed by comparing with the log Marshal-Olkin Weibull Weibull (LMOWW) regression model. The parameter estimates of the regression models are presented in Table 13. The goodness of fit measures of the regression models show that the LHMWW regression model performs better than the LMOWW regression

Table 13: Parameter estimates of the regression models for the hypertension data.

Model	Parameter	Estimate	Standard error	Z value	P value
LHMWW	σ	4.2404	1.0790	3.9298	8.5010×10^{-5}
	α	345.2733	2.8976×10^{-1}	1191.6015	$<2.2000 \times 10^{-16}$
	β	3.2153×10^{-1}	9.2454×10^{-2}	3.4777	5.0570×10^{-4}
	θ	2.6481×10^{-2}	7.2045×10^{-1}	0.0368	0.9707
	γ_0	136.6681	8.1285	16.8134	$<2.2000 \times 10^{-16}$
	γ_1	4.1023×10^{-1}	7.1629×10^{-2}	5.7271	1.0220×10^{-8}
	ℓ= -493.5100	AIC = 999.0204	BIC = 1015.6950	K − S = 0.0487	0.9407
LMOWW	σ	3.5779×10^{2}	1.6212×10^{-2}	22068.5615	$<2.2000 \times 10^{-16}$
	β	7.1405	2.5708×10^{-1}	27.7749	$<2.2000 \times 10^{-16}$
	θ	2.1458×10^{-2}	5.3641×10^{-3}	4.0002	6.3280×10^{-5}
	γ_0	1.3834×10^{2}	5.1886×10^{-2}	2666.1188	$<2.2000 \times 10^{-16}$
	γ_1	9.8022×10^{-1}	2.5966	0.3775	0.7058
	$\ell = 497.4500$	$AIC = 1004.9000$	$BIC = 1018.7950$	$K - S = 0.9644$	$<2.2000 \times 10^{-16}$

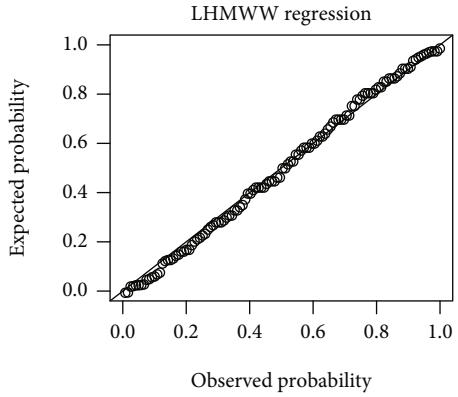

Figure 14: P-P plot of the Cox-Snell Residuals for LHMWW regression residuals.

model. From the parameter estimates of the LHMWW regression model, gender is statistically significant at the 5% level of significance. Thus, the LHMWWW regression results show that the time frame for onset of hypertension is not the same in males and females, and this is evidenced by the significant influence of gender on the survival times of hypertension. This is a revelation of gender differences in relation to time until the onset of hypertension. The finding is useful and consistent with that of Paresh et al. [32].

The likelihood ratio test (LRT) was also performed to compare the LHMWW regression model and the LMOWW regression model. The LRT statistic of 7.8791 with a P value of 0.0050 showed that the LHMWW regression model performs better than the LMOWW regression model.

The Cox-Snell residuals were used to assess the adequacy of the LHMWW regression model. The P-P plot results in Figure 14 show that the LHMWW regression model provides a very good fit to the data set and therefore can be adequately applied for modelling real life data in medical studies.

9. Conclusion

A new family of probability distributions called the Harmonic mixture Weibull-G (HMW-G) family of distributions is introduced in this work. The statistical properties of the family including quantile function, moments, incomplete moment, moment generating function, and mean residual life were comprehensively derived. Five special distributions (HMWBIII, HMWL, HMWW, HMWF, and HMWN) of the family were developed and studied. The density plots of the special distributions showed a wide variety of very attractive shapes making them very suitable for modelling bimodal data sets as well as left skewed, right skewed, and symmetric data sets in medical studies. The hazard function plots also showed a wide variety of shapes making the family very suitable for modelling data with both monotone and nonmonotone failure rates. The maximum likelihood method was used in estimating the parameters of the HMW-G family. The performance of the maximum likelihood estimators was assessed using Monte-Carlo simulation studies. The LHMWW location-scale regression model was developed to investigate the effect of covariates on a response variable that follows the LHMWW distribution. The usefulness of the HMW-G family was demonstrated with applications to real data sets in medicine. The applications empirically showed that the HMWW distribution provides a better fit to the given data sets than the other competing models. Finally, the application of the regression model showed that the LHMWW regression model provided a very good fit to the given data and hence can be adequately applied for modelling data in medical studies. As part of our future studies, sensitivity analysis of the regression model will be performed.

Data Availability

The (blood cancer, diabetes, and hypertension) data used to support the findings of this study are included within the article.

Conflicts of Interest

The authors declare that there are no conflicts of interest regarding the publication of this work.

References

[1] B. Lau, P. Duggal, S. Ehrhardt et al., "Perspectives on the future of epidemiology: a framework for training," *American Journal of Epidemiology*, vol. 189, no. 7, pp. 634–639, 2020.

[2] H. Klakattawi, D. Alsulami, M. A. Elaal, S. Dey, and L. Baharith, "A new generalized family of distributions based on combining marshal-Olkin transformation with T-X family," *PLoS One*, vol. 17, no. 2, pp. 1–29, 2022.

[3] M. A. Aldahlan, F. Jamal, C. Chesneau, I. Elbatal, and M. Elgarhy, "Exponentiated power generalized Weibull power series family of distributions: properties, estimation and applications," *PLoS One*, vol. 15, no. 3, article e0230004, 2020.

[4] S. Nasiru and A. G. Abubakari, "Complementary generalized power Weibull power series family of distributions: estimation and application," *Eurasian Bulletin of Mathematics*, vol. 3, no. 1, pp. 20–37, 2020.

[5] B. Oluyede, P. Mdlongwa, B. Makubate, and S. Huang, "The Burr-Weibull power series class of distributions," *Austrian Journal of Statistics*, vol. 48, no. 1, pp. 1–3, 2019.

[6] M. Ç. Korkmaz, "A new family of the continuous distributions: the extended Weibull-G family," *Communications Faculty of Sciences University of Ankara Series A1 Mathematics and Statistics*, vol. 68, no. 1, pp. 248–270, 2019.

[7] A. Usman, A. I. Ishaq, A. A. Usman, and M. Tasi'u, "Weibull Burr X-generalized family of distributions," *Nigerian Journal of Scientific Research*, vol. 18, no. 3, pp. 269–283, 2019.

[8] M. Ç. Korkmaz, G. M. Cordeiro, H. M. Yousof, R. R. Pescim, A. Z. Afify, and S. Nadarajah, "The Weibull Marshall–Olkin family: regression model and application to censored data," *Communications in Statistics-Theory and Methods*, vol. 48, no. 16, pp. 4171–4194, 2019.

[9] B. Oluyede, "The gamma-Weibull-G family of distributions with applications," *Austrain Journal of Statistics*, vol. 47, no. 1, pp. 45–76, 2018.

[10] M. Ç. Korkmaz, M. Alizadeh, H. M. Yousof, and N. S. Butt, "The generalized odd Weibull generated family of distributions: statistical properties and applications," *Pakistan Journal of Statistics and Operation Research*, vol. 14, no. 3, pp. 541–556, 2018.

[11] H. M. Yousof, M. Rasekhi, A. Z. Afify, I. Ghosh, M. Alizadeh, and G. Hamedani, "The beta Weibull-G family of distributions: theory, characterizations and applications," *Pakistan Journal of Statistics*, vol. 33, no. 2, pp. 95–116, 2017.

[12] A. S. Hassan and M. Elgarhy, "Kumaraswamy Weibull-generated family of distributions with applications," *Advances and Applications in Statistics*, vol. 48, no. 3, pp. 205–239, 2016.

[13] S. H. Alkarni, "Generalized extended Weibull power series family of distributions," *Journal of Data Science*, vol. 14, no. 3, pp. 415–440, 2016.

[14] S. Shafiei, S. Darijani, and H. Saboori, "Inverse Weibull power series distributions: properties and applications," *Journal of Statistical Computation and Simulation*, vol. 86, no. 6, pp. 1069–1094, 2016.

[15] M. Santos-Neto, M. Bourguignon, L. M. Zea, A. D. Nascimento, and G. M. Cordeiro, "The Marshall-Olkin extended Weibull family of distributions," *Journal of Statistical Distributions and Applications*, vol. 1, no. 1, p. 9, 2014.

[16] B. Silva, M. Bourguignon, C. Dias, and G. Cordeiro, "The compound class of extended Weibull power series distributions," *Computational Statistics and Data Analysis*, vol. 58, no. 1, pp. 352–367, 2013.

[17] O. Kharazmi, A. S. Nik, G. G. Hamedni, and E. Altun, "Harmonic mixture-G family of distributions: survival regression, simulation by likelihood, bootstrap and Bayesian discussion with MCMC algorithm," *Austrian Journal of Statistics*, vol. 51, no. 2, pp. 1–27, 2022.

[18] M. Bourguignon, R. B. Silva, and G. M. Cordeiro, "The Weibull-G family of probability distributions," *Journal of Data Science*, vol. 12, no. 1, pp. 53–68, 2014.

[19] S. Kotz and D. N. Shanbhag, "Some new approaches to probability distributions," *Advances in Applied Probability*, vol. 12, no. 4, pp. 903–921, 1980.

[20] I. W. Burr, "Cumulative frequency functions," *Annals of Mathematical Statistics*, vol. 13, no. 2, pp. 215–232, 1942.

[21] K. S. Lomax, "Business failures: another example of the analysis of failure data," *Journal of the American Statistical Association*, vol. 49, no. 268, pp. 847–852, 1954.

[22] W. Weibull, "A statistical distribution function of wide applicability," *Journal of Applied Mechanics*, vol. 18, no. 3, pp. 293–297, 1951.

[23] M. Fréchet, "Sur la loi de Probabilité de l'écart Maximum," *Annales de la Société Polonaise de Mathematique*, vol. 6, pp. 93–116, 1927.

[24] D. R. Cox and E. J. Snell, "A general definition of residuals," *Journal of the Royal Statistical Society: Series B: Methodological*, vol. 30, no. 2, pp. 248–265, 1968.

[25] F. R. S. de Gusmao, E. M. M. Ortega, and G. M. Cordeiro, "The generalized inverse Weibull distribution," *Statistical Papers*, vol. 52, no. 3, pp. 591–619, 2011.

[26] M. H. Tahir, G. M. Cordeiro, M. Alizadeh, M. Mansoor, M. Zubair, and G. G. Hamedani, "The odd generalized exponential family of distributions with applications," *Journal of Statistical Distributions and Applications*, vol. 2, no. 1, 2015.

[27] Y. Amadu, *Some Contributions to Odd Family of Distributions with Applications to Cancer Datasets, [Ph.D. thesis]*, University for Development Studies, 2021, UDSspace, http://www.udsspace.uds.edu.gh/handle/123456789/3319?mode=full.

[28] Y. Amadu, A. Luguterah, and S. Nasiru, "On the odd inverse exponential class of distributions: properties, applications and cure fraction regression," *Journal of Statistics & Management Systems*, vol. 25, no. 4, pp. 805–836, 2022.

[29] H. M. Salem, "The exponentiated Lomax distribution: different estimation methods," *American Journal of Applied Mathematics and Statistics*, vol. 2, no. 6, pp. 364–368, 2014.

[30] M. V. Aarset, "How to identify a bathtub hazard rate," *IEEE Transactions on Reliability*, vol. R-36, no. 1, pp. 106–108, 1987.

[31] A. M. Abouammoh, S. A. Abdulghani, and I. Qamber, "On partial orderings and testing of new better than renewal used classes," *Reliability Engineering and System Safety*, vol. 43, no. 1, pp. 37–41, 1994.

[32] S. S. Paresh, T. L. Greco, and T. Rohr-Kirchgraber, "The sex and gender influence on hypertension," *Health Management*, vol. 19, no. 5, pp. 419–422, 2019.